 © 2013 Russian Academy of Sciences and Turpion Ltd

DOI 10.1070/RC2013v082n01ABEH004329

Nanomaterials and nanotechnologies: methods of analysis and control

I V Gmoshinski, S A Khotimchenko, V O Popov, B B Dzantiev, A V Zherdev, V F Demin, Yu P Buzulukov

Contents

I. Introduction 48
II. Methods for detection and analysis of nanoparticles in multicomponent heterogeneous systems 50
III. Detection of nanoparticles and nanomaterials in the body of laboratory animals by transmission electron microscopy 59
IV. The use of reversed-phase high performance liquid chromatography for fullerene determination in biological samples 63
V. Study of absorption and distribution of engineered nanoparticles in the body of laboratory animals using radioactive tracer method 65

Abstract. The methods for isolation and identification of nanoparticles and for quantitative determination of nanoparticles in complex multicomponent mixed-phase systems are considered. These systems include most environmental objects, in particular, animal and plant organisms, agricultural raw materials, foodstuffs and various sorts of consumer goods. The published data and the results of authors' research concerning determination of various types of nanoparticles in biological samples by electron microscopy, chromatography and radioactive tracer method are generalized. The bibliography includes 161 references.

I. Introduction

Sustainable social development under population growth and environmental deterioration would be globally impossible without implementation of innovative technologies; among these are nanotechnologies defined as the set of methods for targeted manipulation of material items of <100 nm size. Currently, nanotechnologies are regarded as a new industrial revolution.

I V Gmoshinski, S A Khotimchenko Scientific Research Institute of Nutrition, Russian Academy of Medical Sciences, Ust'insky pr. 2/4, 109240 Moscow, Russian Federation. Tel. (7-495) 698 53 71, e-mail: gmosh@ion.ru (I V Gmoshinski), tel. (7-495) 698 53 68, e-mail: hotimchenko@ion.ru (S A Khotimchenko)
V O Popov, B B Dzantiev, A V Zherdev A N Bach Institute of Biochemistry, Russian Academy of Sciences, Leninsky prosp. 33/2, 119071 Moscow, Russian Federation. Tel. (7-495) 952 34 41, e-mail: vpopov@inbi.ras.ru (V O Popov), tel. (7-495) 954 31 42, e-mail: dzantiev@inbi.ras.ru (B B Dzantiev), tel. (7-495) 954 28 04, e-mail: zherdev@inbi.ras.ru (A V Zherdev)
V F Demin, Yu P Buzulikov National Research Centre 'Kurchatov Institute', pl. Akad. Kurchatova 1, 123182 Moscow, Russian Federation. Tel. (7-499) 196 74 03, e-mail: vfdemin_kiae@mail.ru (V F Demin), tel. (7-499) 193 78 83 (Yu P Buzulukov)

Received 23 March 2012
Uspekhi Khimii **82** (1) 48 – 76 (2013); translated by S P Svitanko

The properties of a substance existing as particles of such size differ substantially from the properties of traditional forms of substance, *i.e.*, continuous phases and macroscopic dispersions.[1–4] This is caused, first, by the fact that a substantial portion of atoms or molecules composing the particles are concentrated at interfaces. Second, in some cases, the properties of particles of <100 nm size start to be directly affected by quantum mechanical laws. Therefore, many macroscopically observable properties of nanoparticle (NP) dispersions such as colour, fluorescence excitation and emission wavelengths and so on depend first of all on the particle size rather than on their chemical composition.

The specific properties of NPs open up broad prospects for the targeted manufacture of nanomaterials with enhanced properties — unique mechanical strength and specific spectral, electric, magnetic, chemical and biological parameters.

The application of nanomaterials in modern science and technology is highly diverse. Examples of the key applications are given below:

— materials engineering (development of high-strength structural materials for various fields of industry);

— microelectronics and optics (materials for microchips, computer parts, optical gates, *etc.*);

— power engineering (materials for batteries, fuel cells, high temperature superconductors and so on);

— chemical engineering (development of high-performance catalysts);

— medicine (targeted drug delivery, production of new bandaging materials with enhanced antiseptic properties and new materials for surgery, the development of effective new-generation vaccines);

— scientific research (preparation of labels and tracers);

— environmental control and protection (design of nanochips and nanosensors for the control of various chemical and biological pollutants and remediation of contaminated soils).

It is planned to use nanomaterials for the purposes of genetic and molecular engineering. In the sphere of consumer goods, nanomaterials find use for the manufacture of perfumes and cosmetics and textile goods with antimicrobial properties, personal eye protection devices, sporting goods, household chemicals and many other.[1,5]

Special prospects are opened by nanotechnologies in the food industry.[6–9] Smart packaging materials for foodstuffs are already produced; these materials not only ensure the required antimicrobial properties, particular moisture content and gas permeability, but they are also able to send signals to a consumer about expiry of the product or loss of the acceptable quality. The new types of food additives designed based on nanotechnologies impart various consumer properties (colour, odour, texture) to one and the same product depending on the cooking conditions.[6,10] Of substantial interest is the use of some nutrients (especially minerals, vitamins and bioantioxidants) in the form of NPs or in inert nanoenclosures.[6,7,11–15] This may not only enhance the accessibility of useful components in enriched foodstuffs and biologically active additives but also avoid the chemical or biological incompatibility of nutrients.[6,10] Finally, dispersion of the plant raw materials down to <100 nm particles is considered to be a way of increasing the bioavailability of the flavonoids, microelements and other compounds that are contained there and that can be in deficiency in the human body.

Thus, nanotechnology is obviously among the most promising trends of science and technology of the 21st century. Fast development of the nanoindustry in Russia and abroad and the application of nanomaterials and goods based on nanomaterials in the everyday industrial and domestic practice would result in increasing amount of nanomaterials used by humans, and their discharge to the environment will also grow. Since some properties of nanomaterials have not beed adequately studied, their potentially harmful (in particular, toxic) impact on humans is a topical issue. This problem can be referred to as nanosafety.[1–3,16] Quite a volume of scientific information has been accumulated concerning the biological effects (in particular, toxic action) of practically important nanomaterials such as fullerenes, single- and multi-walled nanotubes, silicon and titanium oxides, silver and gold NPs, quantum dots, nanostructures of polymers and biopolymers; these data were summarized in some review publications.[1–4,17–20]

Studies of nanosafety have been carried out abroad (in the USA and EU) since the early 2000s. In Russia, these studies were started at the end of 2006 under the authority of the Federal Service for Supervision over Consumer Rights Protection and Human Welfare. The initial provision is that nanomaterials should in all cases be classified as new sorts of materials and products, and characterization of the potential risk from these materials for human health and the environment is obligatory.†

† RF Federal laws No. 52-FZ 'On the sanitary and epidemiological welfare of population' and No. 29-FZ 'On the quality and safety of food products'. This statement was reflected in the document 'The concepts of toxicological studies, risk assessment strategy, and methods for identification and quantitative determination of nanomaterials', which was approved by the order of the Russian Federation Chief State Medical Officer of October 31, 2007.[21,22]

A considerable intensification of research and development (R&D) in the field of nanosafety in Russia became possible in 2008 with the start of implementation of the Federal Target Programme 'Development of the Infrastructure of Nanoindustry in the Russian Federation for 2008–2011'. The key investigation results according to this Programme have been generalized in a monograph.[23]

According to this Federal Target Programme, overally 48 regulatory and procedural documents composing a unified hierarchical system of nanosafety in Russia were developed and got approved. Development of this system was initially based on the fundamental statement that nanotechnology should be characterized considering, on the one hand, the potential benefit coming from the application of the products manufactured using this technology and, on the other hand, the safety for humans now and in the future.

The developers of the safety provision system for nanotechnologies and nanomaterials in Russia had to face the same fundamental problems as their colleagues abroad. First of all, this is discrepancy between the multitude of engineered nanomaterials that have been developed and commercialized (by now, >3000) and very slow accumulation of scientific information about their biological properties. A possible way out is to develop a scientifically substantiated method for determining the priority of nanosafety research. This method issued as methodical guidelines, which are based on systematization of published data from scientific literature and resorting to mathematical models, would be suitable for tentative assessment of the potential health and environmental hazard of nano-objects.[16] It is possible to calculate the integrated hazard, which can be classified as low, medium or high. Depending on the hazard class, the scope of necessary toxicological and hygienic research of one or another nanomaterial is defined. Whereas for objects with low potential hazard, only some critical tests are required, for NPs having a high class of hazard, full toxicological and hygienic characterization should be performed whenever possible.

The second important problem faced in the creation of a nanosafety system is to assess the exposure during monitoring and supervision of production, turnover, use and disposal of nanomaterials. Hygienic standardization requires methods for detection, identification and quantification of nanomaterials in environmental objects (air, soil, water, animal bodies, plants — biota components, agricultural feedstock and consumer products). When NPs of a particular chemical composition have been identified in a sample, they should be quantified by means of methods with sensitivity limits at least an order of magnitude lower than the hygienic standard. Also it is highly desirable that this method be able to reliably distinguish between nanomaterials and their chemical analogues as macroscopic dispersions.

During the last decade, this issue was the subject of several reviews and problem papers (see, for example, Refs 24–27) and a monograph (see Ref. 28). However, these papers do not fully disclose and sufficiently detail the aspects of nanoparticle and nanomaterial analysis in biological matrices, in particular, using electron microscopy and isotope tracers.

This review considers the ideas, approaches and methods reported in up-to-date scientific literature related to detection, identification and quantitative determination of NPs and other nano-objects present as parts of complex multicomponent mixed-phase systems, in particular, biological systems.

II. Methods for detection and analysis of nanoparticles in multicomponent heterogeneous systems

1. Preliminary notes

The choice of the analytical method for determination of NPs and nanomaterials is dictated by not only the nature of the subject of analysis but also by the set of most important physicochemical characteristics that are to be determined. The possible biological effects of nanomaterials (both favourable, *i.e.*, nutritive or functional, and adverse, *i.e.*, toxic) are largely determined by the particle size, shape and surface properties.[29] Nanoparticles can be single-component (consist of one compound or element) or multicomponent (have different compounds in different areas or layers). Apart from the chemical composition, the crystal structure and the shape of the particles (especially for inorganic NPs) are significant.[30]

Also, it should be borne in mind that diverse coatings applied onto NPs can be modified (or destroyed) in the body, which can induce unpredictable changes in their properties. This brings about the demand for methods suitable for differentiation between 'native' NPs and their biotransformed derivatives.[29]

A lot of nanomaterials present as parts of biological fluids or complex matrices (such as food products) tend to agglomerate and aggregate.[31, 32] The aggregation of nanomaterials in fluids may result in their precipitation or flotation.[33] The degree and kinetics of aggregation and the size of resulting aggregates depend on characteristics of the particles and dispersion medium and on the particle concentration in the dispersion.[32, 34] The stability against aggregation is an important factor determining the behaviour of a nanomaterial that enters the body as part of a product and influencing the possible toxic impact.[35] The probable formation of aggregates is to be taken into account in the analysis of nanomaterials in natural objects, especially when electron microscopic, spectroscopic, chromatographic methods and ultrafiltration are applied. This is due to the fact that characteristic size and morphological features of aggregated NPs can differ considerably from the corresponding properties of the parent non-aggregated nanomaterial.

The key problem of monitoring of engineered NPs in biological objects is the lack of universal methods or integrated protocols for the analysis by a number of methods able to detect NPs in the objects, locate them exactly at cellular and subcellular levels, identify the detected material, distinguish it from the same substance in macrodispersed or molecular form and quantify the engineered NPs.

When searching for the answer to the question of whether a method is suitable for solving one or another task of those listed above, it is expedient to consider the following characteristics determined by the principles of the method:[36]

— limit of detection;
— complete detection for quantitative determination;
— maintenance of the initial physical state;
— correctness of size measurement;
— probability of false identification of a biogenic nanostructure as NP;
— the presence of common analysis protocols for different NPs;
— applicability for locating NPs in a cellular structure or limitedness to homogenized samples;
— possibility to determine the composition of NPs.

Thus, methods of analysis of nanomaterials should not be limited to gaining simple characteristics such as mass concentration of the analyte or the number of particles in the unit volume but they should also provide information about a set of properties that include shape, size and size distribution, chemical properties of the surface, the presence of trace impurities, stability against aggregation and some other important characteristics.

2. Microscopy and related methods

The procedures based on microscopy comprise optical approaches (confocal microscopy), numerous methods based on electron or X-ray scattering by the samples and a number of techniques known by the common name 'scanning probe methods'.

Typical sizes of NPs (<100 nm) are below the theoretical limit of an optical microscope resolution determined by the visible light wavelength (~ 400 nm).[24] However, the near-field scanning optical microscopy technique lowers the limit of spatial resolution to $\sim 50-100$ nm by means of using an aperture with a diameter smaller than the light source wavelength and thus it can be used in certain cases to detect at least NP aggregates (associates) if not single NPs in the sample.[25]

Light diffraction stipulates the spatial resolution limit of laser scanning confocal microscopy. When this method is used, the spatial resolution limit may be 200 nm. One more distinctive feature of this method is the possibility to study the distribution of fluorescent nanosized objects in the bulk of a rather thick sample owing to high depth of focus. This eliminates many problems related to NP analysis in ultrathin sections inherent in most electron microscopic procedures (see below). An obvious drawback of laser scanning confocal microscopy is the necessity of using fluorescent NPs. Meanwhile, practically valuable nanomaterials possess intrinsic fluorescence only rarely (*e.g.*, quantum dots, some proteins), while most NPs require the introduction of a fluorescent label, which can itself affect the particle surface properties, and this sharply reduces the applicability of the method.[37, 38]

The information content of the light-optical methods in the analysis of NP distribution in biological materials can be increased by using modern automated sample analysis systems.[39]

Electron microscopy methods and the family of scanning probe techniques are used most often for visualization of engineered nano-objects. By using these methods, a resolution down to the subnanometre range can be attained. Atomic force microscopy (AFM) and scanning (SEM) and transmission (TEM) electron microscopy not only provide visualization of single NPs but also give many parameters important for their identifica-

tion and evaluation of their behaviour in a food matrix such as the degree of aggregation, degree of dispersion, size, shape heterogeneity.[40,41] Despite the fundamental difference between the methods applied, the results they provide are often comparable.[24]

Using electron microscopy, it is difficult to determine the structures formed by light atoms (elements from the first and second periods of the Periodical Table) including, which is most important, carbon atoms.[24] However, detection of electron-dense NPs against the background of organic matrix is a routine task for TEM (*e.g.*, see publications[42,43] dealing with determination of distribution of iron, yttrium and zinc oxide NPs in cell cultures).

Electron microscopy techniques can be coupled with analytical techniques providing quantitative information about the chemical composition of the sample. This group of methods was called analytical electron microscopy.[24] Energy-dispersive X-ray spectroscopy can be coupled with SEM or TEM methods; this is suitable for analysis of the composition of samples comprising elements heavier than oxygen with an error of $\sim$20%.[41]

Characteristic electron energy loss spectroscopy (EELS) is based on recording the energy loss of an electron upon running through the sample; this is also suitable for quantitative analysis. EELS techniques can be coupled with TEM, the error of analysis being $\sim$10%.[41,44] Electron diffraction in a selected region can also be coupled with TEM, this provides information about the crystal structure of the particles that form the sample.[44] Using filters that separate zero-loss electrons, it is possible to markedly increase the image contrast. This approach was used[44] to identify multimolecular NPs of C_{60} fullerene in a biological sample without additional contrasting. In another study,[45] this approach provided not only visualization of fullerene particle aggregates in a biological sample but also their high-resolution 3D tomographic images.

The electron microscopy techniques are in the general case destructive, *i.e.*, the sample is destroyed upon investigation and cannot be analyzed once again by another method in order to verify the results. One more drawback is manifestation of electrostatic effects caused by charge accumulation upon passage of the electron beam through the sample. In order to eliminate these effects, an appropriate coating is applied on the sample; however, a considerable part of information about its structure and composition can be lost in this case.

Since the traditional electron microscopy is nearly 'insensitive' to light elements that compose organic compounds, in particular, form the living cell, biological samples should most often be contrasted by compounds of heavy metals (uranium or osmium), which in turn can considerably complicate or even preclude identification of NPs in biological samples. This difficulty can be overcome to some extent by using dark-field scanning transmission electron microscopy. In this case, a satisfactory contrast can be attained for biological objects without additional enhancement. Being coupled with electron diffraction and spectroscopic methods, dark-field scanning transmission electron microscopy provides data on the structures and chemical compositions of various nanomaterials, including those based on organic matter, with a subnanometre resolution.[46] Ustunomiya and Ewing[47] employed high-angle annular dark-field scanning transmission electron microscopy in combination with energy-dispersive spectrometry to characterize heavy metal impurities in amorphous carbon NPs formed upon engine fuel combustion. Richman *et al.*[48] successfully used dark-field scanning transmission electron microscopy to characterize manganese oxide NPs in welding aerosols.

X-Ray microscopy methods can provide spatial resolution of down to 30 nm; this limit is caused by the capabilities of optical devices that focus X-rays. No complicated sample preparation is required; biological samples can be studied in a relatively thick layer without dehydration, fixation or staining.[49] Nurmi *et al.*[50] studied the structure of iron metal NPs synthesized by various chemical methods by X-ray scanning transmission microscopy. X-Ray microscopy techniques can be combined with computer-assisted tomography to obtain 3D images.

A considerable limitation of traditional electron microscopes is that they operate only upon high evacuation of the sample. This rules out examination of liquid samples; the samples have to be dehydrated, cast into epoxide resins or cryofixed. These complicated procedures can produce diverse artefacts.[26] In order to restrict this, various attempts have been made to improve the sample preparation for an electron microscopic study. An example is the cryo-TEM method in which a sample cooled to liquid nitrogen temperature together with the electron microscope chamber is exposed to electrons. This gives rise to the possibility of studying the structure of labile biological samples that would be damaged upon traditional sample preparation. As applied to nanomaterials, this method was used, in particular, by Wang *et al.*,[51] who studied ultrathin TiO_2 particles modified by Fe^{III} in aqueous environment, and by Leppard *et al.*,[52] who studied the behaviour of a variety of practically important NPs and nanostructures in aqueous environment, which concerned viruses, polysaccharide fibrils and iron oxide and hydroxide particles over a broad range of sizes (3 to 500 nm).

Nevertheless, none of the considered methods can completely avoid the artefacts caused by sample dehydration during the sample preparation and investigation. If there is a need to study NPs in their natural (unchanged) surrounding, *e.g.*, in a foodstuff matrix, the use of other techniques may be required. For example, this may be environmental scanning electron microscopy[27] according to which the electron gun and focusing lenses of the microscope occur in high vacuum, while the detector and the chamber with the sample are isolated from the other space of the instrument and can occur at a pressure of $\sim$10 – 50 Torr. This design allows one to investigate the sample in its natural state without dehydration or fixation. The electron beam ionizes the gas phase in the chamber, which ensures the charge flowing off from the sample surface; hence, there is no need to coat the sample with a current-conducting material. One more advantage of the considered method is insensitivity of the detector to disturbances caused by fluorescence and cathodoluminescence. As in the traditional SEM, in the environmental scanning electron microscopy (ESEM), the use of X-ray fluorescence attachment is possible, *i.e.*, the possibilities of energy-dispersive spectrometry are implemented. However, two substantial drawbacks inherent in this method are noteworthy: first,

only a thin surface layer of the sample is subjected to analysis; second, the spatial resolution of ~100 nm does not suffice for visualization of many practically important NPs in non-aggregated form.[24, 27]

The possibilities of traditional SEM and ESEM for the analysis of various colloidal particles in aqueous environment were compared.[53] A comparison of the results of NP visualization in various bottom sediment samples demonstrated that SEM provides much sharper and more high-contrast images than ESEM; however, in the former case, the number of artefacts caused by sample drying markedly increases. The samples studied by ESEM retained their initial morphology to a certain extent; however, obtaining and interpretation of the images were rather labour-consuming. The maximum humidity of the sample was 75%. At 100% humidity, the surface film of water made the visualization of nanostructures impossible. The data on particle size obtained by SEM and ESEM methods were somewhat different. This provided grounds for concluding that both methods are required for detailed characterization of the structures of colloidal particles. Redwood *et al.*[54] used the ESEM method for visualization and quantitative analysis of organic NPs (humic acids) in the bottom sediments of the Savannah river of the south-east of the USA. Analysis was carried out over a broad range of pH (3.3–9.8); a sensitivity of 100 mg dm^{-3} was achieved. The authors arrived at the conclusion that ESEM is more preferred in the studies of hydrated NPs of organic origin; however, this method failed to provide data about the structure of 100% hydrated and absolutely non-perturbed sample.

The wet TEM technique is suitable for examining wet samples, like annular dark-field ESEM; the spatial resolution reaches ~50 nm. A procedure combining elements of TEM and ESEM is suitable, according to its inventors,[55] for investigation of wet samples. When performing the analysis, the grid with applied sample is placed in electron-permeable chamber, which allows examination without vacuum.

WetSTEM capsules were developed for the study of fully hydrated samples using a traditional scanning electron microscope. Two types of capsules were proposed for the use of side-scatter detectors: capsules of one type serve for imaging liquid samples, while the second type is for imaging dense hydrated samples of biological tissues, foodstuffs or soils. This technique allows for detection of NPs directly in the matrices without special sample preparation. The thin film capsule separates the sample from the vacuum chamber of the microscope. The capsule shell is a membrane transparent for an electron flux; this enables imaging at nearly atmospheric pressure. Owing to the use of the capsule, it is possible to connect an X-ray fluorescence spectrometer.[56, 57] The shortcoming of the method is the decrease in the spatial resolution due to distortions caused by the capsule walls and its sensitivity to radiation damage. In addition, the object is discernable only if it directly adjoins the inner surface of the membrane. The theory, analytical characteristics, limitations and the possible applications of WetSTEM capsules in both SEM and ESEM techniques were reported.[58]

An algorithm was proposed [59] for the selection of the TEM procedure for visualization and quantitative determination of NPs in biomaterials. The TEM procedures are surveyed, their scope and limitations are considered in relation to the detection of polystyrene and titania NPs in the respiratory tract of test animals. The authors implied the necessity of biomaterial fixation during sample preparation and subsequent staining.

The fixation mode is determined by the TEM procedure chosen. Note that transition to the NP detection in homogenates and biological fluids eliminates the need to select the sample fixation protocol prior to TEM. After sample homogenization, the bioorganic particles are destroyed by chemical treatment that does not cause NP destruction. This is done using concentrated inorganic acids (nitric or sulfuric), hydrogen peroxide and its mixtures with acids (nitric or sulfuric), or hydrolytic enzyme preparations.

Atomic force microscopy (AFM) is a powerful, rapidly developing method for investigation of nanosized objects, belonging to so-called scanning probe microscopy family.[60] The principle of the method is scanning of the sample surface by an oscillating needle probe so that van der Waals attraction force of about 10^{-12}–10^{-9} N appears between the needle tip and the sample surface. This force depends on the distance between the interacting surfaces; from the change in the probe position (based on laser beam reflection), it is possible to determine the relief of the surface being scanned. Theoretically this may produce the vertical resolution of ~0.5 nm.[61] The lateral resolution is much poorer because particles on the surface of a sample (especially liquid or hydrated one) may shift (drift) upon interaction with the probe tip and even stick to the tip. The oscillation frequency of the probe with the NP stuck to it changes, and this results in artefacts. These unfavourable events can be eliminated by using non-contact scanning in which the sample surface and the tip are separated by a gap.[60]

It should also be borne in mind that the tip size is usually comparable with or considerably greater than the sizes of the analyzed NPs, which inevitably leads to image smearing. As a result, the apparent lateral sizes of particles can be somewhat greater than the actual size. Nevertheless, AFM is suitable for determination of sizes of many practically valuable NPs or even single protein molecules.[24, 27] As applied to analysis of NPs in multicomponent matrices, AFM technique is, first, limited to examination of only the surface of a sample and, second, the traditional AFM fails to give information about the chemical composition of the detected NPs.

Lately, a new AFM version called chemical force microscopy has been developed.[62, 63] The principle of the method is to place molecules that selectively react with the NP material on the probe tip end. For example, to scan the NPs of organic polymers (in particular, proteins), specific antibodies may be placed on the probe tip. Upon the appearance of the specific antigen–antibody interaction, the attraction force between the probe and the surface increases by a large factor, which markedly increases the analysis specificity.[64]

Atomic force microscopy was used to characterize the particles present in natural colloid solutions (water bodies). For example, the results of analysis of such particles and the dependence of their structure on the pH were reported. [65] Mica plates were immersed for 30 min periods into samples preconcentrated by filtra-

tion, then the plates were washed with distilled water and dried prior to the contact investigation. It is noted that scanning of the sample under a layer of the dispersion medium (water) would be perfect. Nevertheless, for sample humidities attained by air drying, the structures of organic colloids adsorbed on the surface were mainly retained. The authors were able to reveal parallelism in TEM and AFM examinations of the samples. Although the AFM examination is possible under atmospheric pressure and ambient humidities, the method may require rather complicated sample preparation procedure,[66] including drop deposition, adsorption, particle deposition and ultracentrifugation. These approaches are thoroughly developed as applied to investigation of natural biopolymer particles, including humic acids and polysaccharides. The issues of using AFM to study nanomaterials utilized in food production were considered in a review.[67]

Scanning tunnelling microscopy is yet another popular version of scanning probe microscopy based on the effect of quantum tunnelling of electrons between the current-conducting tip and the current-conducting surface. The tunnelling current depends on the width of the gap between the tip and the sample; hence, during scanning of the relief surface, the current on the tip varies and this variation is recorded by a sensor. The electronic circuit of the instrument allows the construction of a 3D image of the object. The lateral resolution of a scanning tunnelling microscope is ~ 1 nm.[24] Unfortunately, the classical version of the method is applicable only to conducting (metal or semiconductor) surfaces; therefore, its use for analysis of nanomaterials in food products is problematic. Nevertheless, some recent papers report the application of scanning tunnelling microscopy to biological materials. For example, this method was used[68] to study redox characteristics of bacterial enzymes. In another work,[69] scanning tunnelling microscopy in combination with visible emission spectroscopy and Raman scattering techniques was used to characterize binding of silver NPs to a gold substrate modified by organic adsorbents.

Thus, by combining microscopic procedures, it is possible to visualize NPs and to gain information about their average size, size distribution, chemical and phase compositions and other parameters. It should be borne in mind that analysis and interpretation of electron microscopic images are no less important than the proper electron microscope observation. Almost in all cases, observation is carried out on a thin (or even ultrathin) section of the sample or in a thin surface layer. Hence, the main bulk of the sample is not analyzed, which cannot but affect the statistical reliability of the obtained results. The average particle size being determined is actually a number-average value, and hence it depends on the number of individual particles being examined. When the sample is a complex heterogeneous multiphase system (food product), interpretation of the results of microscopic observations may be difficult. When the sample contains NPs of natural origin, examination of thousands of particles may be required to obtain a reliable result. This calls for necessity of automation of measurements and development of computer programmes for sample analysis. Also, the contrast of the resulting image is not always sufficient for quantitative determination and, as a rule, the presence of solvation shells of NPs that are able to considerably change their behaviour within a matrix cannot be taken into account.

3. Chromatography and related methods

Chromatographic and other related procedures can be used to isolate NP from complex samples. When inductively coupled plasma mass spectrometry (ICP–MS)[70] or voltammetry[71] is used for detection, it is possible not only to determine the contents and parameters of various NPs present in foodstuffs, water, soil or other environmental samples but also to characterize their elemental composition.

Size exclusion chromatography is the best known and most well developed method for the separation of various particles according to their sizes. Columns for size exclusion chromatography are packed with porous beads as the stationary phase. The greater the size (hydrodynamic radius) of the particles, the smaller the number of pores of the stationary phase that are accessible for their penetration, and, hence, the shorter the retention time in the column. This method has been used to study metallic NPs,[72] quantum dots, single-walled carbon nanotubes and polystyrene particles.[73–75] Size exclusion chromatography is distinguished by high separation performance but may give rise to artefacts caused by specific interaction of the fractionated particles with the stationary phase[76] and by the limited range of separation, which does not always cover the range of sizes of practically important engineered NPs or their aggregates.

Size exclusion chromatography can be advantageously combined with various detection methods that are able to estimate the properties of the particles present in particular size fractions, for example, small-angle laser light scattering.[77]

One more method is hydrodynamic chromatography, which also provides the separation of particles according to their hydrodynamic radii. Unlike size exclusion chromatography, in the case of hydrodynamic chromatography, the column is filled by non-porous beads (for example, glass, quartz, polystyrene). The beads form channels in which the particles are fractionated under the action of flow velocity field gradient in the near-wall layer of the stationary phase. When there is a near-wall gradient of the liquid flow velocity, particles are separated according to their hydrodynamic radii: larger particles are eluted faster than smaller particles.[24] The use of non-porous beads substantially decreases the possibility of interaction of NPs with the stationary phase as compared with porous phases. The modern columns for hydrodynamic chromatography are suitable for fractionating particles of various nature in the range of sizes from 5 to 1200 nm. The separation efficiency (the number of theoretical plates) in this method depends on the column length, whereas in size exclusion chromatography the pore size distribution plays the crucial role. Owing to the broader range of size distribution in the case of hydrodynamic chromatography, it is possible to fractionate diverse NPs and their aggregates in various media. The detection in hydrodynamic chromatography can be accomplished by means of fluorescence, ultraviolet and other detectors. These have been used to detect and quantify fluorescent NPs, natural colloids and bio-

polymers.[78–80] Using dynamic light scattering and hydrodynamic chromatography, quantitative determination and size distribution measurement were performed for lipid nanocapsules with diameter of 25–100 nm.[81] The major limitation of this approach is insufficiently high resolution.

Reversed-phase high performance liquid chromatography (RP-HPLC) is currently widely used for detection and quantification of organic compounds. This method is especially convenient for quantitative determination of fullerenes in biological samples.[82,83] The fullerene peak is recorded by a time-of-flight detector or based on UV absorption at the characteristic wavelength of 324–340 nm. For complex samples, sample preparation (extraction with organic solvents) is required. Fullerenes are transferred from the biological material being tested to a nonpolar solvent by means of liquid–liquid extraction. The solvents used most often are toluene or benzene in which C_{60} and C_{70} fullerenes are rather readily soluble up to 1 mg ml^{-1}. A considerable drawback of this method is incomplete extraction in the case of low fullerene contents caused by the formation of stable complexes of fullerenes with proteins and lipids.[82] Therefore, before extraction, biological samples are to be treated with glacial acetic acid or with solutions with high ionic strength in order to destabilize these complexes.[84,85] A simplified version of reversed-phase chromatography of fullerenes in thin layers was reported.[86]

Lately, field-flow fractionation (FFF) technique used to analyze engineered NPs in intricate natural samples has been actively developed.[87] This technique is related to chromatography; however, in this case, fractionation occurs in an open channel without a stationary phase. The particles are separated according to their behaviours in an external force field. The field changes the velocity of particles by forcing them into concentrated laminar liquid layers that move at different rates within an open thin channel. A centrifugal force field (high-speed centrifugation) or hydrodynamic flow field directed at right angle to the main separating flow can be used as the external field. According to the velocity of Brownian motion of particles of various size, they can be fractionated in the range of sizes from 1 nm to 1 μm. According to Tiede *et al.*,[24] FFF is one of the most promising methods for analysis of nano-objects in foodstuffs, in particular, of nanotransporting systems. The instruments for FFF can be equipped with different detectors; in addition, the separated fractions can be analyzed by electron microscopy or by other methods.[88] Field-flow fractionation can be coupled with multiangle laser light scattering and ICP–MS.[89] The scope of applicability of these approaches extends from analysis of natural colloids in fresh and sea water to determination of size distributions of various soil components.[90,91] Dielectrophoretic FFF was used to size-separate single-walled carbon nanotubes[92] and NPs of gold[93] and other metals and also oxides and amorphous carbon.[24]

The limitations of the FFF method are related to the effects of particle interaction with the channel walls (which is especially important for trace or minor components of the analyzed mixture) and the need to perform a complex sample preparation procedure (preconcentration of the initial sample) in some cases. One should also bear in mind that artefacts may appear due to aggregation of NPs in the fractionation channel.[87,94]

Theoretically, both non-aqueous and aqueous phases with broad ranges of ionic strengths and pH (from 2 to 11) can be used as carriers for FFF. By appropriate selection of the eluent, it is possible to minimize the consequences of adsorption of the anatyte on the channel walls and deterioration of the stability of colloidal dispersions.

4. Filtration and centrifugation

Filtration and centrifugation have long been most popular techniques in the toolkit for size separation of various particles. These methods have high speed and productivity; it is possible to handle large numbers of samples. Ultracentrifugation employs centrifugal acceleration of up to 10^6 g as the separating factor. Traditionally ultracentrifugation is classified into analytical and preparative ones. In the analytical ultracentrifugation, the movement of particles in the rotor is recorded on a real-time basis by a UV or refractometric detector. The preparative ultracentrifugation may be implemented in either differential mode (the sample fractions are deposited in the range between lower and higher centrifugal acceleration) or gradient mode [the particles are separated according to their buoyant density in a transformed gradient (aqueous solutions of saccharose) or in a gradient spontaneously formed in the gravitational field (aqueous solutions of caesium chloride)]. The former method is widely used to isolate various biological macromolecules and subcellular structures, in particular, in the nanometre region of sizes.[95]

The membrane filtration methods are classified according to pore sizes of the membranes. Microfiltration is based on the use of membranes with pore sizes from 0.1 to 1 μm, *i.e.*, these membranes are permeable for almost any type of NP (but not for any aggregates).[76] The range of pore sizes from 1 to 100 nm corresponds to ultrafiltration and <1 nm is nanofiltration. Nanofiltration membranes with pores 0.5–1 nm in diameter can be used to concentrate the vast majority of NPs and to separate them from ions of salts and low-molecular-mass organic compounds such as amino acids, simple sugars, *etc*. The principal advantage of ultra- and nanofiltration techniques is that they are suitable for separation of large volumes of samples. In particular, this opens up the possibility to concentrate NP from substantial amounts of water and liquid foodstuffs where they are present in minor quantities.

However, the decrease in the membrane pore size gives rise to increasing number of artefacts associated with the formation of non-mixing layers near the walls and with concentration polarization phenomenon.[96] Due to electrostatic effects, the membrane selectivity can change, and this may lead to overestimation (or underestimation) of the particle size. In order to overcome these problems, tangential filtration and cross-flow filtration[97] techniques were developed; thus, undesirable effects associated with precipitation of the material being filtered, formation of wall films and concentration polarization can be avoided.[76] Currently these are standard methods for the fractionation and preconcentration of colloidal particles both in laboratory and in industry.

Liu and Lead [98] studied the efficiency of NP membrane fractionation by AFM. The authors reported successful concentration of natural colloidal particles with a diameter of up to 12 nm from large volumes of water. The selectivity of isolation was confirmed by atomic force microscope examination of NPs deposited on mica. Successful isolation of organic colloidal particles from the river and lake water by ultrafiltration was reported;[99] fluorescence spectroscopy was used for detection. The efficiency of fractionation of natural and engineered NPs in the size range of 1 – 1000 nm was estimated by cross-flow ultrafiltration.[100] The particle sizes in the fractions were determined by AFM and SEM methods. It was found that the membrane selectivity in aqueous solutions obeys intricate regularities, and the particle size is far from being always the factor responsible for particle penetration through membrane pores. Since NPs have charges and solvation shells, the number of larger particles is overestimated. Since the AFM and SEM methods themselves have, as noted above, a number of limitations, this result should apparently be considered as tentative.

5. Spectroscopy and related methods

A multitude of spectroscopic procedures are used to analyze and characterize the NPs in ordinary systems (dispersions in water and organic solvents). Among the techniques based on scattering, note static and dynamic laser light scattering (DLS)‡ and small-angle neutron scattering.[24]

The DLS method is widely used to determine particle sizes and aggregation degrees in suspensions. Analysis is carried out rapidly, although there are considerable drawbacks.[101] For example, disturbances can be generated by impurities present in the sample such as single micrometre-size dust particles, and this distorts the light-scattering factor from small particles. In addition, considerable difficulties are faced in the interpretation of data from heterogeneous samples (with pronounced scatter of particle size). Using DLS (unlike some other methods), it is possible to gain information on the particle size but not on their chemical composition.[101] As applied to NPs, this method was considerably improved by using transmission grids.[102] This modification is widely used to determine the size distribution in the range of 10 – 100 nm for various types of NPs. Analysis of foodstuff NPs was reported, for example, by Lee *et al.*,[103] who characterized the magnetite (Fe_3O_4) NPs produced by iron-reducing microorganisms, and by Takegami *et al.*,[104] who described the application of the method to study coalescence of lipid nanoemulsions. Murdock *et al.*[105] utilized DLS to characterize aggregation of various engineered NPs (aluminium, titanium, silicon, silver and copper oxide NPs and carbon nanotubes) in various model aqueous solutions of salts and proteins. The investigation results were verified by TEM.

By using static laser light scattering known also as multiangle laser light scattering, one can gain information about the particle structure and by combining this method with DLS and FFF, the particle shape can be determined.[24]

‡ This method is also called photon correlation spectroscopy.

Small-angle neutron scattering is applicable to both solid and liquid samples. In particular, it has been used to characterize the aggregation of natural colloids (fulvic acid) in waste water.[106]

Small-angle X-ray scattering is suitable for characterization of the structures of liquid and solid materials in the nanometre range. It can be used to study both monodisperse and polydisperse systems; in the case of monodisperse NPs, not only particle size but also the shape and structure can be determined.[24]

Among other methods for the analysis of NPs, note laser Raman spectrometry (Raman light scattering) and laser-induced fluorescence. Currently, the scope of application of these methods, which are suitable for detection of NPs in complex miltiphase systems,[107] is limited to the particles bearing definite types of chemical labels. It should be emphasized that these approaches are especially useful for the analysis of some types of organic NPs.[108]

Correlated Rayleigh scattering spectroscopy based on recording the plasmon resonance is used to characterize metallic NPs of >30 nm size. The results obtained by this method were verified using the SEM method.[109]

The isotopes of chemical elements with uncompensated nuclear spin incorporated in NPs can be characterized by NMR spectroscopy. Both particle size and structure can be estimated from the obtained data. Carter *et al.*[110] used this method to determine amorphous silica particles in aerosol and in aqueous dispersion. A version of this method is diffuse NMR spectroscopy, which makes it possible to characterize the particle sizes and aggregation interactions in various colloid solutions.[110, 111] This method was also used to analyze latex nanoparticles.[112]

X-Ray spectroscopic methods comprise X-ray photoelectron, X-ray fluorescence, X-ray absorption and X-ray diffraction spectrometries. A specific feature of X-ray photoelectron spectrometry is the short path length of photoelectrons in the condensed phase; therefore, this method provides information about the composition and structure of a thin (monomolecular at the limit) layer on the particle surface. This gives data about the surface of nano-objects, in particular, about the presence of coatings and adsorbed components.

X-Ray diffraction spectrometry is a non-destructive method suitable for deriving data on the crystal structure and elemental composition of engineered NPs. In combination with X-ray photoelectron spectrometry, this method was used [50] to characterize and quantitatively determine NPs of iron metal and iron oxides meant to be used as adsorbents in waste water treatment.

X-Ray fluorescence spectrometry is also a non-destructive method suitable for elemental analysis of NPs incorporated in multicomponent systems. Two types of this method are wavelength-dispersive and energy-dispersive X-ray fluorescence spectrometries.

X-Ray absorption spectrometry can be used for elemental analysis and selective detection of NPs containing heavy atoms in organic matrices.[24]

Among other spectral methods that can find use for detection of NPs of a particular composition, note electron paramagnetic resonance, Mössbauer spectroscopy, Auger electron spectroscopy and three-dimensional excitation emission matrix fluorescence

spectrometry. Electron paramagnetic resonance is mainly used for detecting NPs bearing a spin label (stable radical). Using Mössbauer spectroscopy, it is possible not only to gain information about the presence of iron-containing particles in the sample but also to elucidate the details of their chemical structure. Three-dimensional excitation emission matrix fluorescence spectrometry was used [99, 113] to identify and quantify organic NPs in river water and industrial effluents.

6. Mass spectrometry

The methods of mass spectrometry are based on separation of charged particles (ions) of different mass in terms of the mass : charge ratio ($m : z$). There exist a large number of mass spectrometric procedures depending on the ion source used, separation principle and the design of detector. The use of mass spectrometry for characterization and analysis of NPs and nanomaterials has two aspects. First, this is a universal method of elemental analysis suitable for high-sensitivity study of the chemical composition of the sample after its cleavage and ionization to single-atom or molecular ions. Second, some approaches allow mass spectral fractionation of some charged heavy multimolecular NPs.

Electrospray ionization (ESI) and matrix assisted laser desorption–ionization (MALDI) can be used to analyze organic compounds present in liquid and solid biological samples. Elemental analysis of metal-containing NPs is performed by inductively coupled plasma (ICP) ionization. The alternative ways of ion separation (ion trap, quadrupole, time-of-flight and magnetic separation), which totally cover a broad range of $m : z$ ratios, differ by the accuracy of mass determination and the attained resolution. All known methods of ion separation are compatible with ESI, whereas MALDI is usually incompatible with quadrupole analysis.[24]

Cai and co-workers [114, 115] considered MALDI with ion trap in combination with laser-induced fluorescence as a method for analysis of polystyrene-based NPs. Also, MALDI was used [116] to detect gold NPs surface-modified by polyoxyethylene groups in cell culture. The sample preparation procedure comprised sample dissolution, transfer of the solution to the substrate, MALDI ionization and analysis of the $m : z$ ratios of the ions thus formed. This design made it possible to identify NPs from the individual mass spectra of the modifying organic molecules.

As noted above, ICP–MS is mainly used for elemental analysis of samples; for example, this may be a useful supplementary tool for detecting metal and metal oxide NPs in biological samples [117] and foodstuffs.[118] In addition, it can be used as a detector in combination with various chromatographic methods. As applied to analysis of nanomaterials, coupling of FFF and ICP–MS techniques is most popular. This approach is highly promising for detection and quantitative determination of NPs in complex matrices, as size-fractionation of particles and determination of the chemical composition of some fractions occur in parallel.[87]

Using the group of single-particle mass spectrometry techniques, it is possible to perform separation and quantitative determination of charged individual NPs. For heavy NPs, very high $m : z$ ratios can be recorded in this way. An example of implementation of this technique is aerosol time-of-flight mass spectrometer. Janzen *et al.*[119] compared the results of investigation of NPs by single-particle mass spectrometry and TEM. Lee *et al.*[120] used single-particle mass spectrometry to estimate the sizes and compositions of polydispersed NPs in aerosol. The results obtained by means of a laser ionization (ablation) time-of-flight single-particle mass spectrometer were verified by a differential mobility analyzer (see below).

7. Particle counting methods

Recently, so-called particle counters started to be used to analyze NPs. One method is based on measuring the change in the electrical conductivity of a weak electrolyte after NPs have been dispersed in it. For increasing the method sensitivity, the sample is passed through a small-size aperture or through a nanosieve, *i.e.*, a membrane with channels formed by multiwalled carbon nanotubes.[121]

According to another method, the size distribution of the NPs suspended in the gas phase (aerosol) is determined using a differential mobility analyzer. First, the particles are charged (*e.g.*, by means of UV- or X-ray-induced ionization) and then their mobility in a uniform electrostatic field is measured. After the measurements, the particles remain suspended in the gas phase, from which they can be isolated to be studied once again by a different method.[24] The particle meter that scans the mobility consists of a differential mobility analyzer and a condensation particle counter. For the investigation, the particles are first separated by a differential mobility analyzer according to the electrophoretic mobility and then the numbers and the sizes of particles in the condensation particle counter module are determined.[24]

Particle counting methods are applicable only to NPs suspended in the gas phase; hence, they are hardly applicable to analysis of foodstuffs. However, currently analogous approaches are being developed for NP dispersions in liquids of charged species. A combination of dynamic light scattering and mobility in a uniform electric field underlies functioning of the Zeta Sizer instrument (Malvern Instruments, UK), which has been utilized, for example, to study the size distribution and the charge of the electric double layer of the lipid NPs meant for oral administration into laboratory animals (rats).[122] A similar instrumentation was used [123] for quantitative determination and measurement of aggregation of titanium dioxide (rutile) NPs in various model and biological media.

8. Adsorption and thermodynamic methods

Determination of the true surface area of NPs is a complicated task, because methods based on direct size determination (TEM, SEM, AFM) may ignore the porosity of particles and the presence of subatomic surface roughness and thus underestimate the target value. The specific surface area of powdered nanomaterials is determined most often by the classical Brunauer–Emmett–Teller (BET) method based on inert gas adsorption isotherms.[24] However, the technical aspects of applicability of this method to analysis of NPs isolated from complex matrices have not been adequately elaborated by now.

The NP phase changes including melting, crystallization, rearrangement of the crystal structure, hydration–dehydration can be studied by highly sensitive thermogravimetry and differential thermal analysis. When coupled with mass spectrometry, thermogravimetry can be used for analysis of the chemical properties of NP surface. On heating, the shells surrounding the particle core are vapourized one layer after another and the material thus formed is subjected to mass spectral analysis. This approach could find use for identification of some special types of engineered NPs.[24]

9. Electrophoresis

In electrophoretic methods, separation is based on the difference between the ξ-potentials of the electric double layer, while in the case of electrophoresis in a support medium, also based on particle sizes. These methods have long become classical for fractionation of biopolymers (proteins and nucleic acids) but as regards application to NPs in complex multicomponent matrices they are still under development.

Engineered NPs can be heterogeneous in the ξ-potential; hence, they can be fractionated in terms of the electrophoretic mobility. An example of application of electrophoresis in a support medium for characterization of the NPs present in foodstuffs was reported in a study[124] dealing with the electrophoretic mobility of silicon dioxide NPs in aqueous salt solutions with different ionic strengths. The electrophoretic fractionation of gold NPs modified by DNA macromolecules was performed.[125] Unlike electrophoresis in a support medium or size exclusion chromatography, in capillary electrophoresis the NPs being fractionated do not interact with the stationary phase matrix. Capillary electrophoresis is suitable for charge and size separation of NPs in various solvents. The presence of at least these two factors determining the mobility hampers interpretation of the results. In addition, there is still the possibility of interaction between the particles and the mobile phase. The application of this method is exemplified by size separation of engineered NPs of gold and its alloy with silver[126] and characterization of colloidal particles of humic acids and other natural polymers.[127]

10. Immunochemical methods

Immunochemical analysis based on interaction of the compound being determined with specific antibodies is a promising approach for detecting NPs. The immune complex formed can be detected if a detectable label such as enzyme, fluorophore, isotope, *etc*., is introduced in one of the immunoreagents. Advantages of immunochemical methods include selectivity and the possibility to detect the target compound in a non-fractionated multicomponent sample and to analyze several samples simultaneously. However, the preparation of antibodies against NPs, which lack typical antigen determinants, unlike natural biopolymers, may face with difficulties.

The preparation and the properties of anti-dendrimer antibodies have been reported.[128] The methods for preparation of mono- and polyclonal antibodies to fullerenes and the procedure of enzyme-linked immunosorbent assay (ELISA) for water-soluble derivatives of these compounds were described.[129, 130]

Hendrickson *et al*.[131, 132] continued the studies dealing with immunodetection of fullerenes in various samples. The immunoreagents for detecting C_{60} — conjugates of C_{60} fluorescently labelled with proteins and poly- and monoclonal anti-C_{60} antibodies — were characterized. The specificity of the resulting antibodies with respect to various classes of carbon NPs was studied. Monoclonal anti-C_{60} antibodies were found to have cross reactivity with C_{70} fullerene and multiwalled carbon nanotubes. The ELISA and fluorescence polarization immunoassay procedures for determination of C_{60} and C_{70} fullerenes and carbon nanotubes were developed for the first time. It was demonstrated that the developed enzyme-linked immunoassay is suitable for determination of C_{60} in organ homogenates of rats after intraperitoneal and intragastric exposure to this fullerene. Fullerene C_{60} was extracted from biological samples into toluene and then the fullerene-containing extract was transferred to a water-organic mixture.

The immune interaction is not the only option of molecular recognition of nanoparticles. The creation of artificial receptors for fullerenes based on various compounds was reported.[133, 134] The affinity of ligand–receptor interaction is comparable in some cases with the affinity of the fullerene–antibody interaction.

11. Limitations of the modern methods of analysis of nanomaterials

We have considered the key methods applied to characterization and quantitative determination of NPs. The vast majority of these methods have been elaborated to date only for pure NPs or their dispersions in ordinary media (gases, single-phase liquids) and they cannot be directly used to examine multicomponent, multiphase, optically non-transparent systems such as foodstuffs.[27] It was noted above that for determination of the contents of NPs in various media, it is insufficient to merely gain information about their mass concentration or even the number of particles. Important characteristics that affect the properties of a highly dispersed substance are also the particle size distribution, the NP shape, surface area and surface structure. None of the existing methods is able to provide full information about the NPs; hence study of NPs (in particular, those present in foodstuffs) should be integrated; selection of a particular investigation method should depend on the nature of both the target particles and the matrix.

Many of the existing analytical tools starting with electron microscopy and ending with dynamic light scattering and field-flow fractionation are theoretically suitable for integrated estimation of NP parameters; however, their application to complex multicomponent systems is limited to a few examples. The difficulties may be brought about by the presence of several types of engineered and natural NPs in natural samples. One more problem is related to the fact that most methods are destructive, which always precludes independent verification of their results.[27] The interaction of NPs with an intricate matrix is also a source of all sorts of artefacts. For example, the aggregation of initially monodisperse NPs, which occurs in natural media, may give rise to aggregates with sizes ranging from tens of nanometres to several tens of micrometres.[105, 135] Therefore, DLS, size

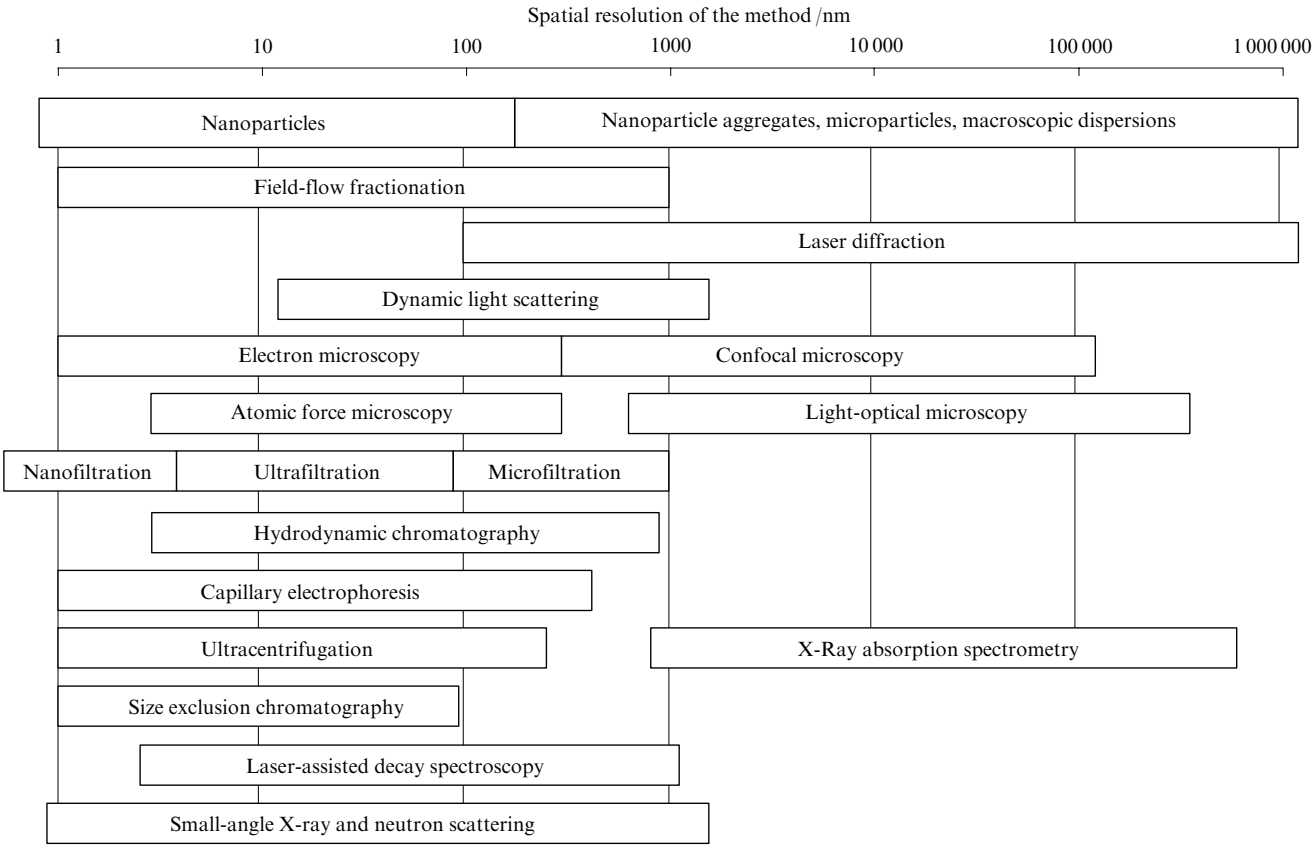


Figure 1. Scope of applicability of the methods providing information on the sizes of NPs incorporated in complex matrices.

exclusion chromatography, ultrafiltration and so forth are inapplicable to these samples.

Modern methods for NP detection and quantitative determination can be classified into two types: those applicable to single particles (depending on their size) and to large bulk of the sample. Elemental analysis techniques (such as ICP–MS) refer mainly to the second type, although it is possible to find approaches suitable for analyzing the composition of single particles. The first type of methods, which mainly includes all of the considered microscopic procedures, provides information on the size, shape and properties of single particles; however, the application of these methods to items incorporated into a complex matrix is hampered, which is manifested as insufficient sensitivity and high probability of false-negative results. These statements are illustrated by Fig. 1, which shows the block diagram reflecting the applicability of various groups of methods to analysis of natural objects with allowance for the attained spatial resolution.

12. Artefacts caused by interaction with the matrix and reference sample problems

The limitations of each method can lead to results inconsistent, first of all, in the important parameter such as particle size in the matrix of a natural object. Correct determination of nanoparticle sizes is complicated by artefacts depending not only on the analytical method applied but also on the nature of the product in which the investigation is performed. For example, the presence of adsorbed components on the particle surface and solvation shells composed of light atoms invisible in an electron microscope accounts for sharp discrepancy between the results of TEM measurements, on the one hand, and FFF or DLS measurements, on the other hand.[101] This especially refers to analysis of inorganic NPs in protein solutions because it is known that an extended protein 'crown' can be formed on the particles under these conditions.[72, 136]

Yet another important problem is the absence of reliable standard reference samples of NPs and nanomaterials.[76] Currently researchers have to use, instead of such samples, commercially available samples, which often lack adequate characterization. Therefore, an urgent task is to develop reference samples[§] and standardized sampling methods and methods of analysis of environmental specimens (in particular, foodstuffs) for the presence of potentially dangerous NPs.[1]

13. Sample preparation problems

The environmental specimens examined for the content of engineered NPs and nanomaterials should be sub-

§ The Joint Research Centre of the European Commission arranged in 2011 the first storage of nanomaterials and started, in cooperation with the Institute of Reference Materials and Measurements, the manufacture and release of certified standard nanomaterials.

jected, depending on the used method, to more or less intricate sample preparation procedure to preconcentrate NPs and nanomaterials and separate them from the matrix components, which can distort the investigation result or preclude the investigation. In the vast majority of cases, sample preparation includes transfer of the sample into the water-soluble state. The composition of the dispersion medium surrounding the NPs considerably changes, which can affect the particle size, composition and structure and thus distort the results.[137–139] These problems can be avoided by using the techniques that do not require sample preparation; however, they are often unavailable.

If sample preparation cannot be avoided, the procedure must be tested using standard nanomaterial samples, and the possible modifications of the nanomaterials should be followed in each step of treatment. Nanoparticle aggregation or, conversely, dissolution under the action of reagents used in the sample preparation may occur. For example, for practically important (in the case of foodstuffs) nanomaterials such as zinc oxide, zero-valent iron, iron oxides and magnesium oxide, the use of mineral acid solutions is impossible, except for the cases where the elemental composition of the sample is to be determined, due to the possible complete dissolution of NPs. When sample preparation involves micro- and ultrafiltration, fast aggregation of the NPs isolated from foodstuffs can occur in aqueous, water–salt and water–protein solutions,[27, 105] which is to be taken into account for membrane selection based on the pore size.

When morphological methods are used (such as electron microscopy), the researcher has to make efforts to preserve the sample structure as fully as possible during the sample preparation. A number of approaches have been elaborated to achieve this goal ranging from encapsulation of the sample into a gel for SEM examination of microemulsion samples[140] to freeze drying of biological samples prior to TEM examination.[54, 101] Fixation methods are also being elaborated for AFM examination of samples; they are suitable, in particular, for analysis of nanoclay samples in aqueous dispersion.[26]

14. Elucidation of the origin of nanoparticles

Yet another problem is to prove the man-made origin of nano-objects detected in the sample.[24] Currently it is very difficult to reliably establish the difference between engineered NPs and nanometre-size particles of natural or technogenic origin, which may also be present in the sample.[137] A multitude of solid particles of <100 nm size are present in the environment. Some of them may have resulted from processes that occur in nature (volcanic eruptions, forest fires) and some other may have formed upon combustion of automotive and aircraft fuel, fuel oil and coal at fuel-burning power plants, garbage at garbage recycling plants, *etc.*[141–143] Nanoparticles dissipate in the environment and can get into food as contaminants. Generally, the problem of differentiated determination of engineered and natural NPs has not yet been solved. Obviously it would be expedient to study representative sampling of foodstuffs that are knowingly manufactured without nanotechnologies in order to estimate the background contents of NPs of one or another type in these products. A task of this sort was solved in a study[118] where the background contents of titanium dioxide were determined by ICP–MS for a broad range of foodstuffs present in the USA and Japan markets; this allowed determining these NPs in food using elemental analysis.

15. Labelled particles

Labelled NPs are conveniently employed to detect NPs in environmental objects (for example in animal bodies).[144] This procedure can be used successfully in a variety of model experiments — to study migration of nano-objects from the packing into the food product, their absorption in the gastrointestinal tract and distribution in the body of test animals and transfer along the trophic chains in model ecosystems.[19, 145, 146]

The introduction of isotope (stable or radioactive) tracer into NPs is the method most consistent with research goals. The possible associated changes of physical and chemical properties of nanomaterials are minimized. Analysis of labelled particles requires mere determination of the amount of the isotope by either ICP–MS (for stable isotopes) or γ- or β-spectrometry (for radioactive isotopes). For some stable isotope tracers (for example, ^{13}C) and for iron isotopes, other methods of detection are available, for example, NMR, magnetic resonance imaging,[147, 148] Mössbauer spectrometry (resonance absorption of γ-quanta). This can be performed without destroying the sample.[24] Using labelled particles, it is possible to study a living organism without disturbing its vital activity, which is of particular interest for biological tests.

Chambers and Mitragotri[149] used ^{3}H-labelled polystyrene NPs. Other examples of using this type of labels were also reported.[19, 150]

By using fluorescent labels, it is possible to visualize NPs in biological media, for example, using confocal microscopy.[24, 142, 150] The uptake of fluorescently labelled NPs in cells can be studied by flow cytofluorometry.

Compounds that produce a characteristic signal in the Raman spectra constitute a specific type of labels. Currently these labels are used to study engineered NPs; moreover, they can be detected directly in the body of a laboratory animal.[107] Flow cytofluorometry with laser excitation can also be used for recording Raman spectra.[109]

The possibilities provided by various types of labelling for toxicological studies were surveyed in reviews.[19, 135]

III. Detection of nanoparticles and nanomaterials in the body of laboratory animals by transmission electron microscopy

The supervision of production, turnover, use and disposal of nanomaterials and hygienic regulation of the contents of engineered NPs in the environment requires methods capable of detection, identification and quantitative determination of such NPs. It was noted above that electron microscopy is the most developed and reliable method for detection and identification of engineered NPs. Using this method, it is possible to determine the particle number, size, and shape for electron-dense compounds in the 1 to 100 nm range of sizes within complex multicomponent and multiphase matrices

such as natural specimens (*e.g.*, biological tissues or single cells). The supplementary option —electron diffraction in the chosen area — provides information about the presence of crystal structure and a definite chemical composition in the NP; this is valuable information useful for NP identification.

Below we present our results of application of transmission electron microscopy for analysis of penetration of engineered NPs into organs and tissues of laboratory animals from the gastrointestinal tract. A model method of NP introduction close to physiological conditions was used, in particular, the NPs were introduced into an ileal segment isolated by sutures with undisturbed blood circulation and nerve supply. The electron-microscopic examination was carried out after fixation of small fragments of tissues or organs in a solution of glutaraldehyde and postfixation in osmium dioxide. The ultrathin sections were produced after dehydration and enclosing of the fragments into epoxy resin. The ultrathin sections were analyzed without a contrast agent.

The detection and identification of NPs were performed successively: first, the electron-dense images were taken, then the electron diffraction from the chosen area was obtained. Nanoparticles can be identified based on reference electron diffraction patterns measured for reference samples.

The following samples of nanomaterials were used.

1. The concentrate of high-dispersion (cluster) silver Argovit (produced by the research and production centre Vector-Vita, Russia). The sample was an aqueous dispersion of silver NPs containing 1.0 mass %– 1.4 mass % of Ag and 18.6 mass % – 19.0 mass % of polyvinylpyrrolidone (PVP) with molecular mass of 15 – 30 kDa as the stabilizer. A TEM examination showed round, ellipsoidal and irregular-shaped silver NPs with an average diameter of 34.9 ± 14.8 nm; the minimum size of the detected particles was 8.4 nm and the maximum size was 80.9 nm.

2. Titanium dioxide (rutile) nanoparticles (produced by Sigma-Aldrich, USA, Germany). According to TEM examination, the rutile NP sample was composed of partially aggregated 40 – 50 nm-long rod-like nanocrystals 5 – 10 nm in diameter.

The study was carried out on 12 male Wistar rats weighing 200 ± 20 g who received balanced casein-based semisynthetic diet. Titanium dioxide (rutile) NP and silver NP dispersions with 50 and 1 mg cm^{-3} concentrations, respectively, in an isotonic NaCl solution were prepared. Dispersions (up to 5 cm^3) were introduced into the silk sutures-isolated ileal loop of rats under hexenal anesthesia for a period of 3 h. After this period, the isolated ileal loop with Peyer' patch, a hepatic lobe and the spleen were separated under deep hexenal anaesthesia. The samples were immediately immersed into solutions of glutaraldehyde and subjected to electron-microscopic examination.

The obtained biological material was divided into two portions. One portion was fixed only with glutaraldehyde and the other was postfixed with a 1% solution of OsO_4 (in 0.1 M phosphate buffer) for 2 h at room temperature to identify the location of NPs in particular tissues and structures of the particular organs. Then the test and control samples were dehydrated in ethanol of increasing concentration and in acetone and embedded into the EPON-812 epoxy resin. The sections were produced by an LKB-3 ultramicrotome (Sweden), and no additional contrasting was used. The ultrathin sections thus obtained were applied on grids coated by a formvar film and examined by a JEM-100C electron microscope. The chemical nature and the crystal structure of the detected NPs were studied by electron diffraction (only for the glutaraldehyde-fixed material).

In the obtained images, nanoparticles were identified by morphometric features and by electron diffraction from the chosen area, the NPs were counted, the number of NPs per unit section area was determined, the distribution and location of the NPs were characterized on the cellular and subcellular levels and NP positions relative to the main cell organelles were described. On contrasted sections, damages of cell ultrastructures were noted.

1. Analysis of engineered nanoparticles in animal tissues ¶

a. Titanium dioxide nanoparticles

Single titanium dioxide NPs (average size of 25 – 30 nm) and numerous large NP aggregates (size of 50 to 500 nm) were detected in the small intestine lumen of rats (Fig. 2*a*). Single NPs were found on the surface and

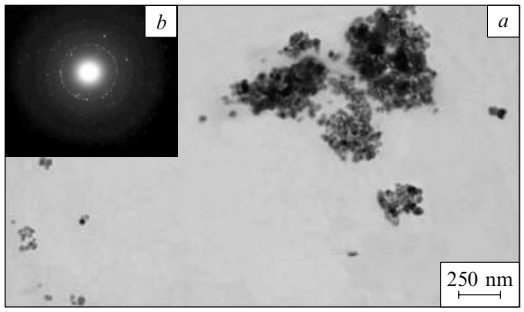


Figure 2. Electron photomicrograph of TiO_2 nanoparticle aggregates (25 – 30 nm) in the small intestine lumen of a rat (*a*) and diffraction pattern of nanoparticles (glutaraldehyde fixation) (*b*).

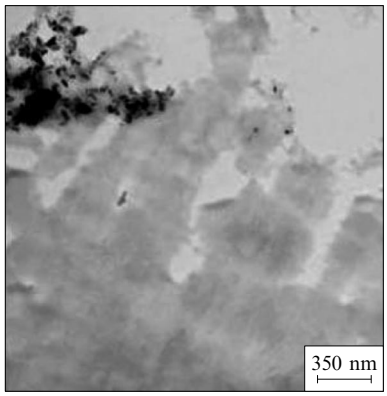


Figure 3. Electron photomicrograph of TiO_2 nanoparticles in the small intestine mucosa of a rat on the surface and between the villi of the small intestine mucosa enterocytes.

¶ The photomicrographs to this section were produced by S M Pridvorova and T A Platonova (A N Bakh Institute of Biochemistry of the RAS).

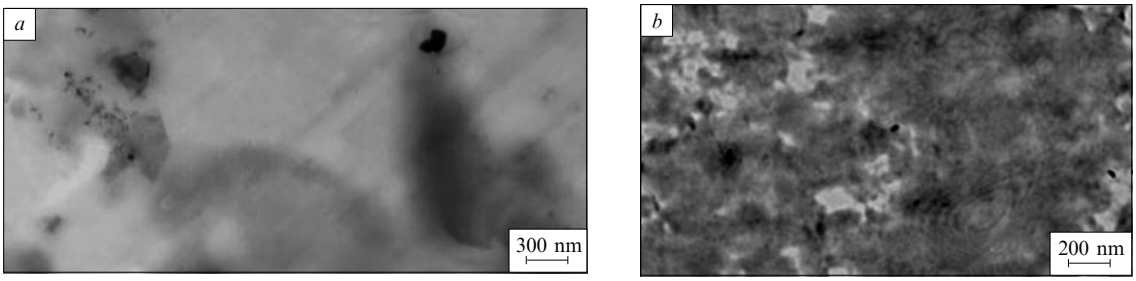


Figure 4. Electron photomicrographs of TiO_2 nanoparticle aggregates (25 – 30 nm) in the section on the mucosal surface (*a*) and inside the tissues (*b*) of the small intestine.

between the villi of the small intestine mucosa (Fig. 3) and inside the epithelial layer of the mucosa (Fig. 4 *a*,*b*). For the glutaraldehyde-fixed material, we failed to determine the exact intracellular localization due to the poor contrast of the image. The presence of titanium dioxide NPs in the sample was confirmed by the presence of separate reflections and diffraction rings (see, for example, Fig. 2 *b*).

In the OsO_4-postfixed material, NPs of 25 – 30 nm size were detected not only in the villi sections (Fig. 5 *a*) but also in deeper layers of the mucosa, particularly, in the muscular layer of the intestinal mucosa (Fig. 5 *b*,*c*). Also, in this case, NPs were observed inside cells (near mitochondria).

Analogous patterns of intratissue localization of titanium dioxide NPs were obtained in electron-microscopic examination of the small intestine Peyer's patches

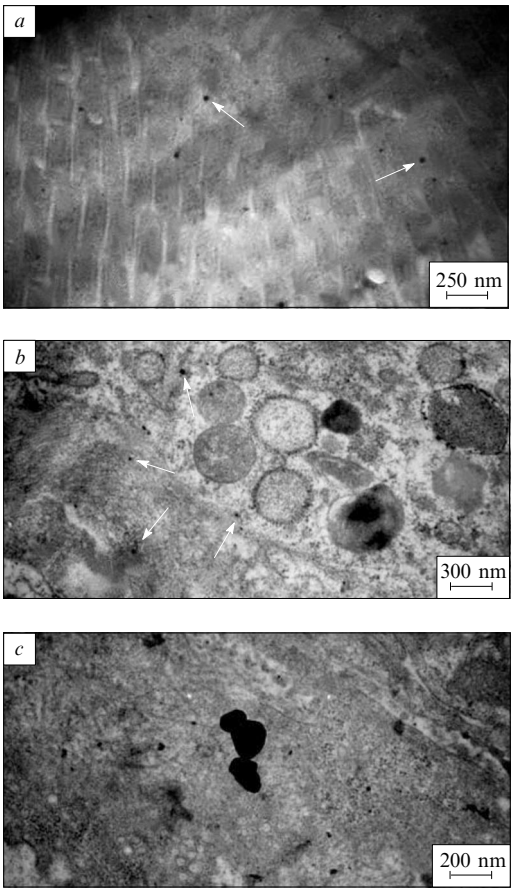


Figure 5. Electron photomicrographs of TiO_2 nanoparticles (25 – 30 nm) in the longitudinal section of villus enterocytes (*a*), in the section of a muscle plate layer (*b*) and in the section of mucosal tissues (*c*) of small intestine (glutaraldehyde and OsO_4 fixation).

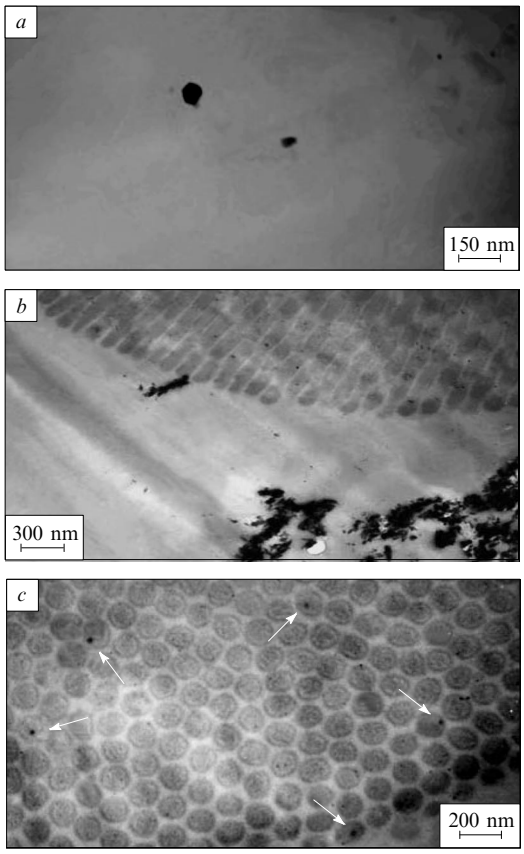


Figure 6. Electron photomicrographs of TiO_2 nanoparticle aggregates (25 – 30 nm) in the section of the Peyer's patch surface of the small intestine (*a*) and longitudinal (*b*) and transverse (*c*) sections of the epithelial cell microvilli on the Peyer's patch surface of the small intestine (glutaraldehyde and OsO_4 fixation).

(Fig. 6). In the case of only glutaraldehyde fixation, NPs are visualized but it is impossible to determined in what cellular structures they occur. In the case of double fixation (glutaraldehyde and OsO_4), single NPs inside the cells near organelles are visualized in the micrographs (see Fig. 5 *c*).

These data are consistent with the published results of electron-microscopic examination of titanium dioxide NPs in the rat intestine mucosal enterocytes.[151] Thus, electron microscopy is capable of detecting the penetration of titanium dioxide NPs from the small intestine lumen into the mucosa, both in the epithelial layer and deeper layers.

b. Silver nanoparticles

The results of electron-microscopic examination of the sections of tissues of animal internal organs after enteral tube intraintestinal administration of a silver NP dispersion were reported.[152]

The preliminary experiments did not detect any electron-dense inclusions in any of the tissues of control animals.

Analysis of the ultrastructure of tissue sections of test animals after introduction of silver for glutaraldehyde-fixed samples confirmed the penetration of NPs into all of the studied tissues. Electron-dense particles of 10 to 120 nm sizes were detected in the small intestine mucosa and Peyer' patch sections both inside and outside the tissues. The presence of silver NPs in small intestine tissue sections is confirmed by the diffraction pattern (Fig. 7).

In the glutaraldehyde-fixed material, fine ($\sim$30 nm) and coarse (up to 100 nm) silver NP aggregates were observed in the liver hepatic cell cross-section (Fig. 8) and in cell cytoplasm. It can be seen that the nanoparticles are located near or between the rough endoplasmic reticulum canaliculi. The resulting diffraction patterns of NP aggregates depending on their localization (on the surface or inside the sections) look like smeared rings (if the aggregate is inside the section) (see Fig. 8 *a*) or separate reflections (if the particles occur on the section surface).

The photomicrographs of the tissue fragments of spleen red pulp with the detected single silver NPs of different size (20–30 nm) and their aggregates (40–90 nm) are presented in Fig. 9. The diffraction pattern of these NPs confirms the presence of silver NPs both on the section surface (separate reflections in the electron diffraction pattern) and inside the section (smeared rings in the electron diffraction pattern).

Thus, the results of electron-microscopic examination demonstrated the presence of silver NPs of various size and different configurations in the organs and tissues of rats after administration of aqueous dispersions of these particles into the small intestine lumen under nearly physiological conditions. The detected nanoparticles were located in many intracellular structures: in cytoplasm, nuclei, endoplastic reticulum membranes, in normal mitochondria and in megamitochondria. Comparison of the experimental electron diffraction patterns with a reference diffraction pattern obtained from a standard silver NP sample confirmed the crystalline nature of the found NPs.

The results demonstrated that upon administration of aqueous dispersions of silver NPs into gastrointestinal tract (by a short-term three hour contact) the particles can penetrate through the small intestine mucosal epithelium into other organs of the animal, in particular, into liver and spleen. This fact should be taken into account for estimating the possible risk of NPs for humans.

The results presented in this Section confirm the efficiency of transmission electron microscopy for the detection and identification of NPs in biomatrices upon NP penetration from the gastrointestinal tract.

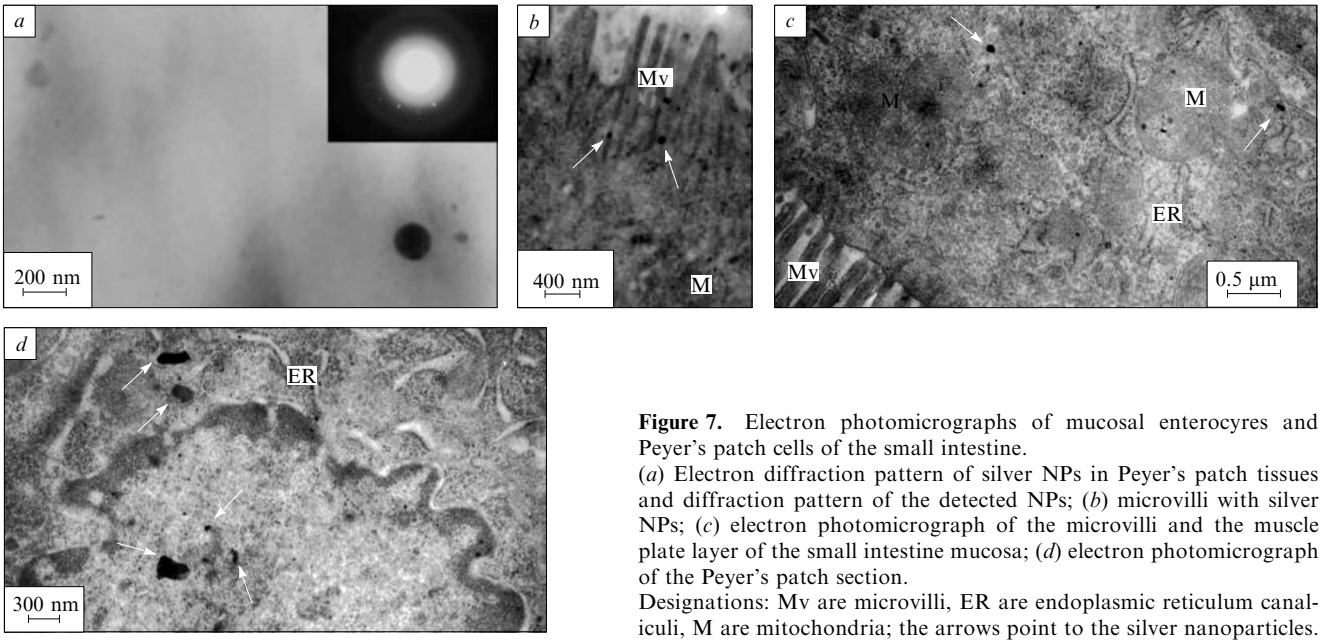


Figure 7. Electron photomicrographs of mucosal enterocyres and Peyer's patch cells of the small intestine.
(*a*) Electron diffraction pattern of silver NPs in Peyer's patch tissues and diffraction pattern of the detected NPs; (*b*) microvilli with silver NPs; (*c*) electron photomicrograph of the microvilli and the muscle plate layer of the small intestine mucosa; (*d*) electron photomicrograph of the Peyer's patch section.
Designations: Mv are microvilli, ER are endoplasmic reticulum canaliculi, M are mitochondria; the arrows point to the silver nanoparticles.

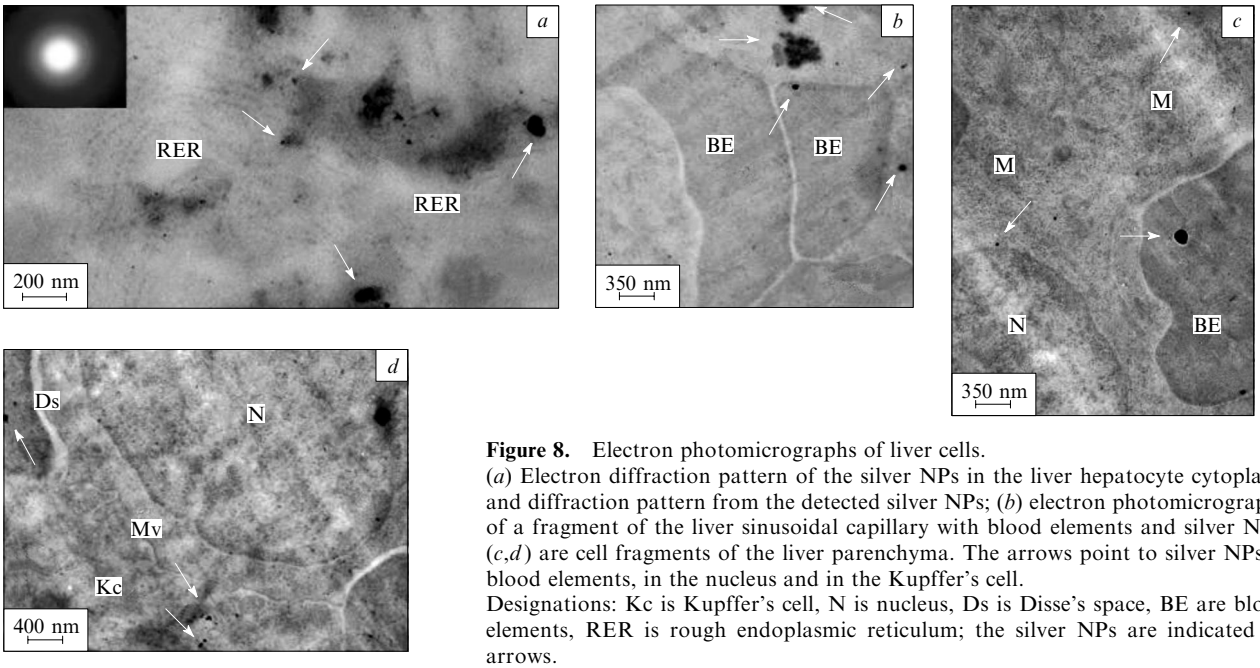


Figure 8. Electron photomicrographs of liver cells.
(*a*) Electron diffraction pattern of the silver NPs in the liver hepatocyte cytoplasm and diffraction pattern from the detected silver NPs; (*b*) electron photomicrographs of a fragment of the liver sinusoidal capillary with blood elements and silver NPs; (*c*,*d*) are cell fragments of the liver parenchyma. The arrows point to silver NPs in blood elements, in the nucleus and in the Kupffer's cell.
Designations: Kc is Kupffer's cell, N is nucleus, Ds is Disse's space, BE are blood elements, RER is rough endoplasmic reticulum; the silver NPs are indicated by arrows.

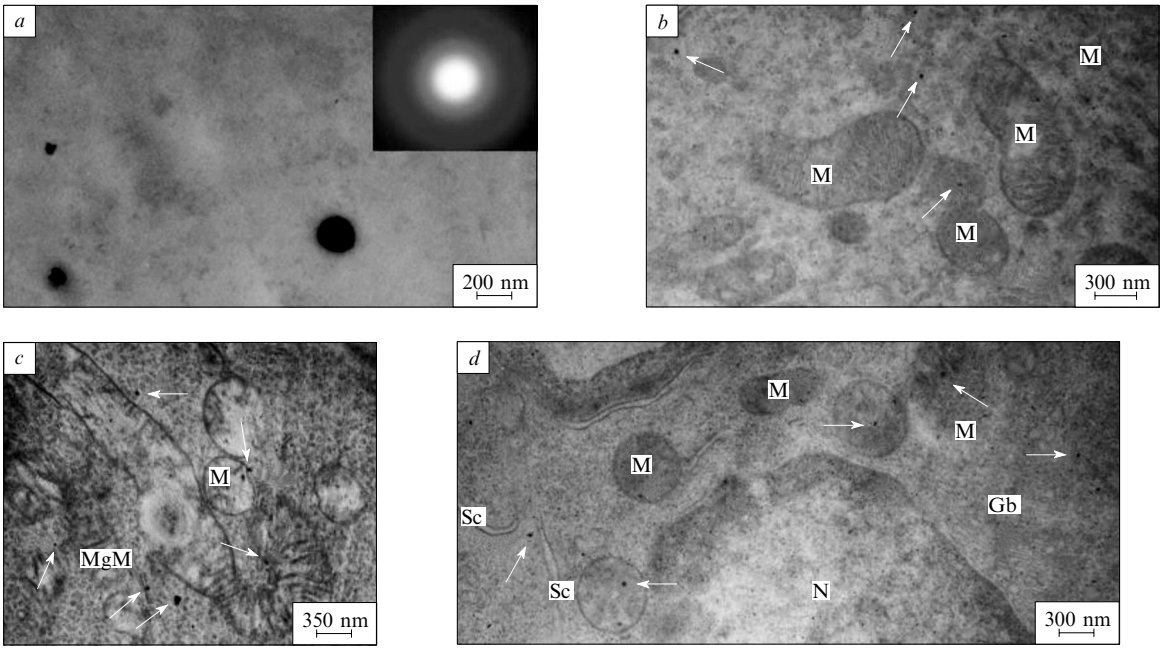


Figure 9. Electron photomicrographs of reticulum cells of the spleen red pulp.
(*a*) Electron diffraction pattern of silver NPs inside and outside the spleen red pulp tissue and diffraction pattern from these nanoparticles; (*b*, *c*, *d*) electron photomicrographs of the reticulum cells of the spleen red pulp with silver NPs in cell mitochondria, cytoplasm and nucleus. Designations: MgM are megamitochondria, Sc are sinusoidal capillaries, Gb are Golgy bodies. The arrows point to silver NPs.

IV. The use of reversed-phase high performance liquid chromatography for fullerene determination in biological samples

Quantitative determination of non-modified C_{60} fullerene in the organs and tissues of experimental animals after its oral administration was performed by HPLC with optical recording. The animals were administered C_{60} fullerene as a single dose or daily for 30 days in an amount of 50 or 250 mg per rat weighing 250 g. The quantitative determination of fullerene in the toluene extracts of organ and tissue homogenates† was done on a Stayer high-pressure liquid chromatograph (Akvilon, Russia)

† Liver, kidneys, brain, spleen, lungs and intestine homogenates were kindly provided by the Institute of Physiologically Active Compounds of the RAS.

with spectrophotometric detection. The components of the toluene extract of biological samples were separated on a Diaspher-110 C18 reversed-phase column (250 × 4 mm) assembled with a Guard Cartridge Starter Kit Kromasil 100-5C18 column (BioKhimMak-ST, RF).

Quantitative determination of C_{60} fullerene in toluene can be performed by spectrophotometry as the fillerene has rather high solubility and high molar extinction coefficient in this solvent. Figure 10 shows the absorption spectrum of C_{60} fullerene in toluene.

The limitations of the spectrophotometric method for quantitative determination of C_{60} fullerene in the extracts of biological samples are mainly related to the effect of the biological matrix (or its components) on the spectral characteristics of C_{60} solutions in toluene. Therefore, prior to the quantitative analysis of C_{60} in biological samples, it is necessary to separate all components of the toluene extract. The method of choice for this purpose is RP-HPLC.

The C_{60} concentration in biological samples from laboratory animals may be very low. Therefore, in the sample preparation it is necessary to maximize the fullerene extraction and to use highly sensitive detection methods. In order to maximize the extraction, an advanced sample preparation procedure was proposed according to the block diagram shown in Fig. 11. Acetic acid increased the solubilization of proteins and other

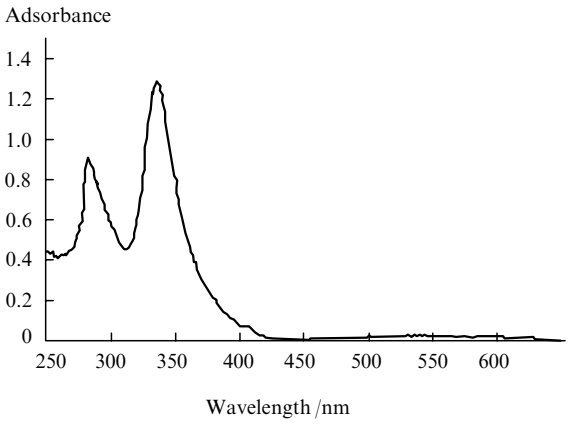
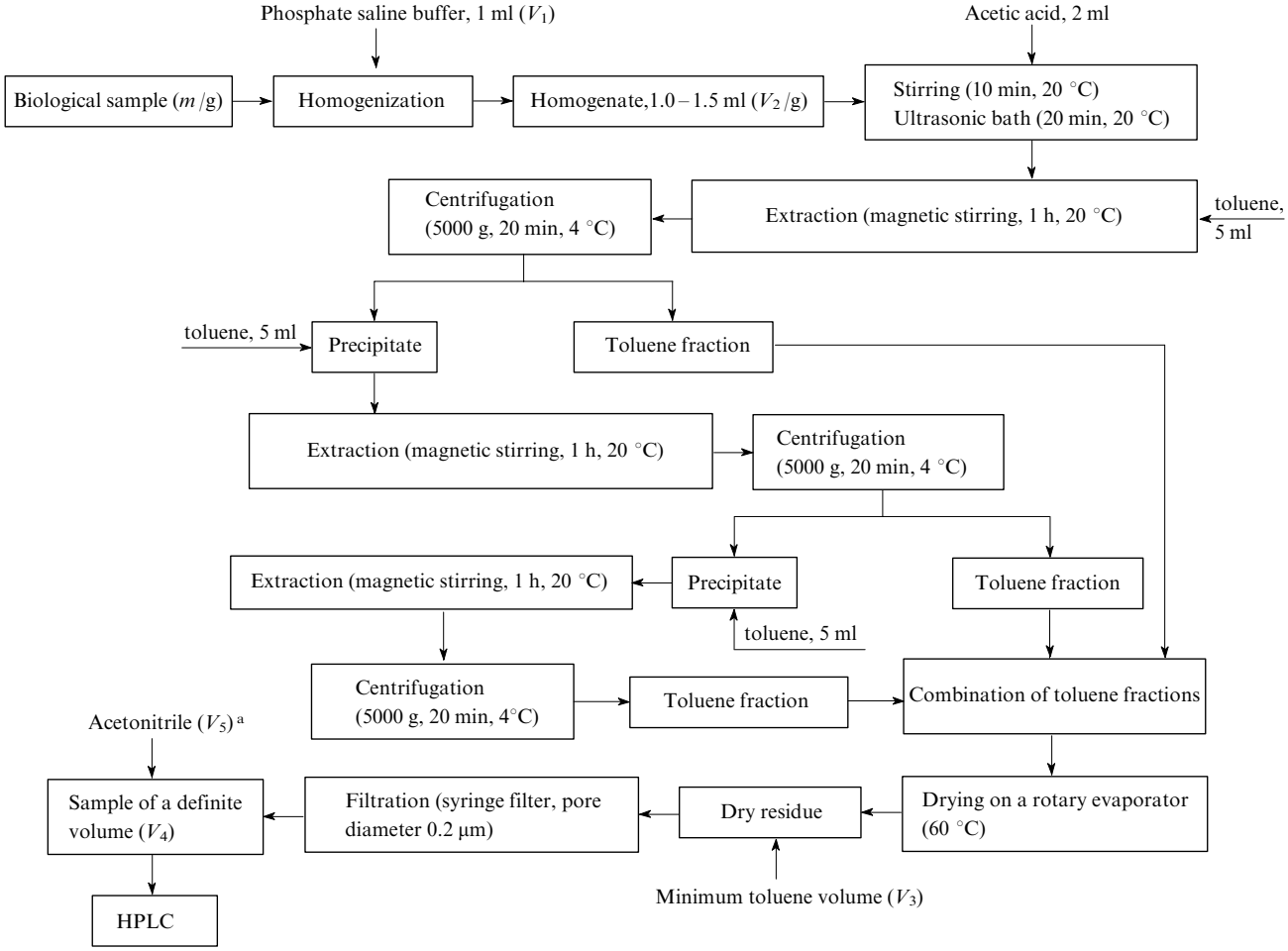


Figure 10. Absorption spectrum of fullerene in toluene. $[C_{60}] = 16\ \mu g\ ml^{-1}$.



[a] To a toluene : acetonitrile ratio of 60 : 40 (vol.%)

Figure 11. Block diagram of the sample preparation procedure for quantitative determination of fullerene in homogenates by HPLC.

surfactants in biological samples. The C_{60} extracts of biological samples were dried by evaporation on a rotary evaporator at 60 °C. The sample preparation included the following stages:

— sampling and sample homogenization in a phosphate saline buffer (pH 7.4);

— treatment with glacial acetic acid in an ultrasonic bath;

— three extractions of the homogenized sample into toluene;

— separation of the precipitated biomatrix by centrifugation after every extraction;

— combining the toluene fractions and drying on a rotary evaporator;

— dissolution of the dry residue in a known amount of toluene;

— filtering the sample through a Teflon filter (pore diameter 0.2 μm);

— dilution of the sample with the chromatographic mobile phase.

The chromatogram of the standard sample of C_{60} fullerene is presented in Fig. 12.

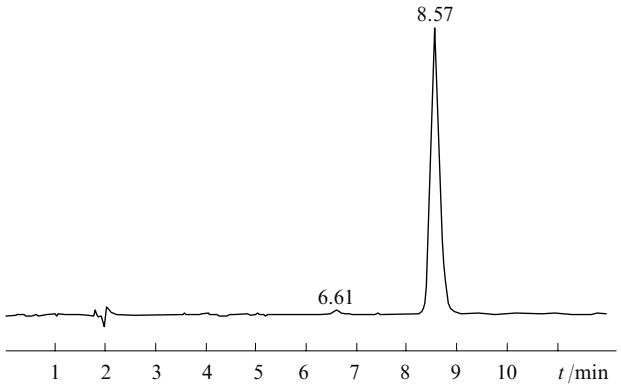


Figure 12. Chromatogram of the C_{60} reference sample.

The 'added–found' experiments demonstrated that the degree of extraction of fullerene from homogenates of various tissues is 90%–95%.

The amount of C_{60} in tissue homogenate samples was determined from the calibration dependence of the C_{60} peak area in the chromatogram *vs.* fullerene concentration in the analyzed sample plotted beforehand. The plot was linear in the C_{60} concentration range from 0.1 to 3.5 μg ml^{-1}.

The chromatograms of the toluene extracts of the homogenates of organs of experimental animals exhibited in some cases smeared peaks (which may refer to modified C_{60}) at nearly the same retention times. The possibility of modification of C_{60} in the animal body was demonstrated.[153] The authors analyzed the C_{60} modification products in the mice liver by various physicochemical methods and demonstrated that C_{60} is functionalized by vitamin A.

It was found experimentally that after single-dose administration of C_{60}, reliably no fullerene accumulation is observed in rat lungs, intestines, brain, spleen, liver or kidney. After daily administration for 30 days, C_{60} was detected in the kidneys of 50% of the laboratory animals on the 7th and 18th day of the experiment at a 250 mg dose, in the intestine of one rat on the 7th day and one more rat on the 30th day of the experiment and in the lungs of one rat on the 30th day of the experiment at a dose of 50 mg per day.

V. Study of absorption and distribution of engineered nanoparticles in the body of laboratory animals using radioactive tracer method

Study of absorption, distribution in the body, metabolism and excretion of NPs is an important stage in the evaluation of safety of NPs and nanomaterials. As applied to main types of engineered NPs, these studies are called upon to solve the following principal problems:

— elucidation of the mechanisms and quantitative estimation of the penetration of NPs and nanomaterials into the body for natural administration routes (oral, percutaneous or inhalational);

— detecting the organs and tissues able to accumulate engineered NPs and, hence, being potential targets of their toxic action;

— qualitative and quantitative characterization of the excretion of nano-objects out of the body, estimation of their retention as a possible indication of cumulative action;

— study of the metabolism of NPs and nanomaterials in the body, which is important for both elucidating the possibility of natural detoxification and evaluating the prospects of using NPs as sources of nutrients of medicine.[2, 19, 24, 27]

The solution of these problems is difficult mainly due to inadequately developed methods for highly sensitive and specific determination of NPs in complex biological samples (see above). It was noted previously that a possible way to solve this problem is to use various labels, of which radioisotope tracers can be named as universal labels.

Radioactive tracer method (RTM) as applied to evaluation of organotropism and biokinetic characteristics of NPs implies the introduction of radioisotope-labelled NPs into the animal body and the subsequent measurement of the radioactivity of organs and tissues. By using the RTM, one overcomes the shortcomings inherent in other methods such as electron microscopy, atomic force microscopy and elemental analysis. These shortcomings are related to insufficient sensitivity and specificity of NP detection in complex mixed-phase multicomponent biological entities. The radioisotope tracer itself does not affect the chemical and surface properties of NPs and does not change noticeably their organotropism and cumulative potential. In view of the high sensitivity of the modern radiometric instrumentation, radioisotopes of very low activity, below the minimum significant activity stipulated by the radiation safety standards operating in Russia, can be used in experiments.‡

‡ See Sanitary Rules and Standards 2.6.1.2523–09 (radiation safety standards 99/2009).

Owing to high selectivity of γ-spectrometery, RTM can be used as simultaneous administration of several sorts of labelled NPs bearing different radioisotope tracers in one and the same animal. Then it becomes possible to comparatively estimate the organotropism and biokinetic characteristics of NPs with higher reliability.

The RTM is most applicable to the study of distribution and organotropism of the NPs that are insoluble in biological liquids and are slowly metabolized in the body. These are numerous metal particles (silver, gold, platinum group metals), non-metals, metal oxides and some salts.

The key limitation of the method is that the NPs must contain an element able to be activated in a (thermal or fast) neutron flux to give radionuclides having quantum energies and half-lives acceptable for γ-spectrometry. A considerable extension of the range of NPs may be achieved by using more complex activation methods on charged-particle accelerators (protons or γ-quanta with energy above the threshold of photonuclear reactions) and by using neutron radiation analysis for detecting the isotope label.[154]

As applied to soluble and (or) biotransformable NPs (active metals, iron, zinc and other oxides), RTM can also provide comprehensive information about their fate in the body. However, in this case, for detecting the specificity of the behaviour of nanomaterials as compared with the traditional analogues, it is desirable to use additional methodical approaches, in particular, to characterize the chemical nature of the biotransformation of labelled NPs using, for example, various chromatographic procedures.

1. Introduction of radionuclide tracers into nanoparticles

The following key neutron activation reactions for elements that compose the NPs under investigation were used:[13, 155]

thermal neutron activation by reaction of (n,γ) type

$$^{109}Ag + n \longrightarrow {}^{110m}Ag, \quad (1)$$

$$^{74}Se + n \longrightarrow {}^{75}Se, \quad (2)$$

$$^{197}Au + n \longrightarrow {}^{198}Au, \quad (3)$$

$$^{64}Zn + n \longrightarrow {}^{65}Zn; \quad (4)$$

fast neutron activation by reaction of a (n,p) type

$$^{46}Ti + n \longrightarrow {}^{46}Sc, \quad (5)$$

$$^{47}Ti + n \longrightarrow {}^{47}Sc. \quad (6)$$

The nuclear constants and other data characterizing the above-indicated initial and activated isotopes are summarized in Table 1.

For the successful use of a desired procedure in biological experiments, it is necessary that the radioactive products of neutron activation of the initial stable isotopes have a half-life ranging from several days to several hundred days (radionuclides with longer half-lives are less active, which reduces the accuracy of measurements). The use of radioactive isotopes with a half-life of less than 24 h causes considerable technical difficulties in the measurements.

The isotopes used in the experiments described below complied with these requirements and were obtained by thermal neutron activation on an IR-8 nuclear research reactor or by fast neutron activation on a cyclotrone at the Kurchatov Institute Research Centre.

Reactions (1)–(4) occur in a thermal neutron flux (the energy range of the thermal neutrons $0.005 < E_n < 0.4$ eV). No titanium radioisotopes of the required lifetimes were present in thermal neutron reactions. For this reason, the ^{46}Sc and ^{47}Sc tracers formed from stable isotopes ^{46}Ti and ^{47}Ti, respectively, in the fast-neutron threshold reaction (n,p) (with proton ejection) were chosen.

Table 1. Characteristics of initial and activated Ag, Se, Ti, Au, Zn isotopes involved in neutron capture and γ-activity measurement (according to the IAEA nuclear database; www.iaea.org/Our Work/Nuclear Data Service).

Nano-material	Isotope of the target				Radioactive isotope				
	isotope	natural abundance (%)	M /g mol^{-1}	$\sigma \times 10^{-24}$ /cm^2	radioactive isotope on n-capture	$T_{1/2}$ /days	type of radiation	E_γ /MeV	n_γ /decay^{-1}
Silver	^{109}Ag	48.2	108.91	4.4	^{110m}Ag	249.8	β$^-$, γ	0.6577, 0.8847	0.95, 0.73
Selenium	^{74}Se	0.9	73.92	48.0	^{75}Se	119.8	γ [a]	0.2647, 0.1360	0.59, 0.61
Titanium dioxide	^{46}Ti	8.3	45.95	0.01	^{46}Sc [upon (n,p) reaction]	83.8	β$^-$, γ	1.1211, 0.8892	1.0, 1.0
	^{47}Ti	7.4	46.95	0.01	^{47}Sc [upon (n,p) reaction]	3.4	β$^-$, γ	0.1594, 0.9835	0.68, 1.0
Gold	^{197}Au	100	196.97	98.7	^{198}Au	2.7	β$^-$, γ	0.4118	0.96
Zinc oxide	^{64}Zn	48.6	63.93	0.6	^{65}Zn	244.3	β$^+$, γ	1.115	0.51

Note. Designations: M is the isotope atomic mass, σ is the neutron capture cross-section, $T_{1/2}$ is the isotope half-life, E_γ is the isotope γ-radiation energy, n_γ is the quantum yield (the number of photons per decay).

[a] On the capture electron reaction.

The radioactive nuclei ^{46}Sc and ^{47}Sc isomorphically replace some titanium nuclei in the crystal lattice of titanium dioxide. Since the atomic radii of these two elements do not differ much, this apparently does not cause any significant distortion of the crystal lattice or change in the physicochemical and biological properties.

The following nanoparticles were used in the experiments:

— silver NPs as Argovit (produced by the research and production centre Vector-Vita, Russia), which were characterized above;

— titanium dioxide NPs as rutile (produced by Sigma-Aldrich, USA, Germany), which were characterized above;

— spherical gold NPs of a 8 nm average size prepared by a reported procedure [156] in the presence of sodium citrate;

— selenium NPs obtained at the Wave Research Centre of the A M Prokhorov General Physics Institute of the RAS by ablation of a compact target made of reagent grade elemental (red) selenium in deionized water without surfactants;[157] according to electron microscopy data,[158] the average particle size was 65 nm;

— zinc oxide NPs (produced by Sigma-Aldrich, USA, Germany) with an average diameter of 28 – 30 nm according to photon-correlation spectrometry data.

For neutron activation, the NP samples (dry powders of zinc oxide and titanium dioxide NPs, aqueous dispersions of silver, selenium and gold NPs) were sealed into ampoules made of extra-pure (99.99%) quartz. The NPs for neutron activation should not contain significant amounts of sodium ions, as upon activation, sodium isotopes can be formed and interfere with determination of the target radioactive tracers. Therefore, gold NP samples containing solutions of sodium citrate were subjected, prior to sealing, to long-term dialysis in sacks of the Visking cellulose membrane (Serva, Germany) with a pore size of $\sim$1 nm against a 10^{-2} mol dm^{-3} solution of reagent grade citric acid.

For the radioactive tracer procedure, the NPs under study with a specified isotope tracer activity were orally (through an enteral tube) administered into the animals. The activity was chosen to achieve a compromise between the radiation safety requirements (the amount of the radioactive sample present at the workplace should not exceed the level defined as the minimum significant activity in the above-mentioned standard) and the technical capability of the γ-spectrometric instrumentation.

The neutron activation session in a thermal neutron flux was carried out as follows. The sealed quartz ampoules with the material to be irradiated as ultradisperse powder or aqueous suspension containing a specified amount of the NPs to be studied were placed into unsealed containers made of extra-pure aluminium. For irradiation, the containers were sunk into the vertical channel of an IR-8 reactor on a aluminium link chain (5 m-long lower part) and a polethylene fish line (5 m-long upper part) to a depth corresponding to the neutron flux maximum.

After the irradiation, the container was pulled up to a level 2 – 3 m above the active zone and left inside the bioprotection for 'cooling', *i.e.*, decay of most of short-lived radioisotopes, in particular, ^{28}Al with $T_{1/2} = 2.7$ min and ^{31}Si with $T_{1/2} = 2.6$ h, which are responsible for the predominant radiation exposure during the first hours after irradiation. After 'cooling down' for several days, the sample containers were taken out of the bioprotection under the supervision of a dosimetrist. The resulting radioactive powders or aqueous suspensions were diluted by deionized water to form specimens to be administered into test animals.

The neutron activation session of titanium-containing NPs in a fast neutron flux was performed in the following way. A sample of the initial dry ultradispersed titanium dioxide powder placed into a polyethylene container was irradiated with fast neutrons in a special channel of a cyclotrone at the Kurchatov Institute Research Centre. Fast neutrons were generated in the cyclotrone by irradiating a beryllium target with a proton beam with an energy of up to 30 MeV. The (p,n) reaction of ^{9}Be isotope yielded neutrons with an energy of 14 ± 6 MeV.

After irradiation with a neutron flux, aqueous suspensions of silver and selenium NPs were diluted down to concentrations of 1 and 50 μg cm^{-3}, respectively. The irradiated zinc oxide and titanium dioxide NP powders were dispersed in water to concentrations of 2.5 and 77 μg cm^{-3}, respectively. Due to the very high specific radioactivity of the gold isotope, the aqueous suspension was diluted, after irradiation with a neutron flux, to a concentration of 5.8 μg cm^{-3}.

2. Procedure of the biological experiment

The organotropism and biokinetic characteristics of the NPs were estimated using male Wistar rats with body weight of 200 – 300 g, who received the standard semi-synthetic diet.

The radioisotope-labelled NPs were administered intragastrically as a single dose. The administered NP doses and the activities of isotope tracers are summarized in Table 2. Immediately prior to administration into the animals, the dispersion of labelled nanoparticles was sonicated (44 kHz, 250 W acoustic power) for 15 min in a water ultrasonic bath to reduce the particle aggregation level.

Table 2. Administered nanoparticle doses and isotope tracer activities.

Rat weight /g	NP	NP dose /mg	Isotope tracer	Isotope tracer activity /kBq
200	TiO_2 (rutile)	77	^{46}Sc	1.75
	TiO_2 (rutile)	77	^{47}Sc	81.8
	Zn	1.25	^{65}Zn	48.8
250	Ag	1	^{110m}Ag	25.1
300	Au	5.8	^{198}Au	53.9
	Se	0.105	^{75}Se	15.05

Immediately after the administration of the NP dose, the animals were placed in cages designed to enable separate collection of faeces and urine. Throughout the stay in the cages the rats had unrestricted access to food and drinking water. The faeces and urine were collected on the first, second, third and fifth days after administration of the specimens. The animals that were administered a particular test material were divided into 3 or 4

subgroups, each comprising four rats. The biological samples were taken on the first day after administration from the animals of the first subgroups of all test groups, on the second day from the second subgroup animals, on the third day from the third subgroup animals, on the fifth day from the fourth subgroup animals after exsanguination from the inferior vena cava under deep ether anaesthesia. The radioisotope activity was analyzed in the following biological samples: whole blood, liver, spleen, pancreatic gland, gonads, kidneys, lungs, heart, brain, gastrointestinal organs, musculoskeletal frame with hair and skin. The materials placed in polyethylene sealed tubes were stored before the measurements in containers made of extra-pure polyethylene at -20 °C.

Then the fabricated samples were studied on a γ-spectrometric instrumentation to determine the activity of the radioisotope tracer by selective measurement of one (or several) γ-energy lines inherent in the particular isotope (Table 3). By summing up the sample activities for each rat, the integrated activity of the isotope tracer was determined for each animal taking into account the activities of the daily amounts of faeces and urine excreted from the animals before sample withdrawal. The integrated value thus obtained was correlated with the introduced dose, and the ratio of these values was used to estimate the accuracy of measurements.

Table 3. Distribution of ^{46}Sc and ^{47}Sc tracers in the body of rats at various time intervals after intragastric administration of ^{46}Sc- and ^{47}Sc-labelled titanium dioxide NPs (in percent of the administered dose, $M \pm m$).

Biological specimen	Time after administration /h		
	24	48	72
GIT [a]	79.2 ± 10.4	1.68 ± 0.24	0.125 ± 0.063
Carcass [b]	0.055 ± 0.016	0.040 ± 0.016	0.020 ± 0.004
Liver	$<2 \times 10^{-3}$	none	none
Blood	$<2 \times 10^{-3}$	the same	the same
Faeces	20.7 ± 10.4	98.30 ± 0.23	99.90 ± 0.06

[a] Gastrointestinal tract. [b] The skin and hair coat and the bladder were also included in the musculoskeletal frame.

3. Measurement of the sample activity

The activity of the samples was measured on a low-background γ-spectrometer manufactured by Canberra (USA) comprising a GC4018 semiconductor extra-pure germanium detector, a DSA-1000 analyzer and Genie 2000 – Genie S501 and Genie S502 software. According to the procedure of measurements, the γ-radiation quanta from the test sample were registered (counted) over a broad energy range in which the operator adjusted either manually or automatically the range of the appropriate characteristic spectral line that was chosen for measurements of the tracer isotope for the subsequent treatment (decoding). The full spectrum of each measured sample was recorded and retained for the repeated treatment or for reference.

During treatment, the count rate of γ-quanta in the chosen energy range was calculated and then converted to the absolute activity of the sample (in becquerels) with allowance for recording efficiency correction factors, in particular, in conformity with the source (biological sample) geometry. For all radioisotopes, the measured activity was additionally corrected for radioactive decay by conversion to the instant of administration of the labelled NPs in animals ($t = 0$). An additional correction of the measured activity of the withdrawn blood and frame weight was applied to account for the incomplete exsanguination, the actual blood weight being taken to be 6.0 % of the body weight.

4. Investigation results

a. Titanium dioxide nanoparticles labelled by ^{46}Sc and ^{47}Sc radioisotopes

The presence of two radioisotope labels, ^{46}Sc and ^{47}Sc, formed upon neutron irradiation of TiO_2 nanoparticles gives a noticeable advantage for the analysis of biological samples with γ-activities differing by several orders of magnitude (this is the case when the gastrointestinal absorption is low, which is typical of this type of NPs). The simultaneous recording of γ-activities of both isotopes presented no difficulty, and the highly active but rapidly decaying ($T_{1/2} = 3.4$ days) ^{47}Sc isotope was used during the first days after administration of labelled NPs for measurement of samples with low NP contents. The less active but long-lived ^{46}Sc isotope suited for measurement of faeces, gastrointestinal tract and frame with high contents of NPs for a long period of time (up to several months) without considerable influence on the accuracy and sensitivity of the method. The highest sensitivity of the applied method in the analysis of NP distribution among organs and tissues, ~0.8 μg for a labelled NP sample, was attained using ^{47}Sc. The balance of determination of the tracer radioactivity was, on the average, (108 ± 5)%, which is within the accuracy of the method for the given isotope. As follows from the data of Table 3, the main bulk of the titanium dioxide NP tracer was located the first day in the gastrointestinal tract and later it was almost completely excreted with the faeces. The degree of tracer excretion after three days was 99.9%. Minor (<0.06%) quantities of the tracer detected in the frame could be due to faeces remaining on the skin around the anus. After the first 24 h, a very low (about 0.002%) radioactivity from ^{47}Sc was detected in the liver and blood of the animals; this corresponded to a titanium dioxide NP contents of ~0.8 μg. No activity of labelled TiO_2 nanoparticles was revealed in the spleen, pancreatic gland, gonads, kidneys, lungs, heart, brain or urine, *i.e.*, the contents of NPs in these biological specimens did not exceed 0.001%.

The results demonstrated that titanium dioxide NPs show low absorption from the small intestine. This does not contradict the data of electron microscopy, which revealed only a few NPs of this type in the enterocyte cytoplasm after introduction of a nanomaterial dispersion into the intestine lumen (see Section III.3.a and Ref. 151). Earlier experiments [14] showed the presence of slight amounts (~4 μg for the whole organ) of TiO_2 (rutile) nanoparticles in the liver of rats after daily administration of high doses of these NPs for a month, which does not contradict the result of our study.

Table 4. Distribution of ^{110m}Ag in the body of rats at various time intervals after intragastric administration of the ^{110m}Ag-labelled silver NPs (in percent of the administered dose, $M \pm m$).

Biological specimen	Time after administration /h		
	24	48	72
GIT + faeces (the sum)	> 98	> 98	> 99
Carcass	0.36 ± 0.17	< 0,6	0.23 ± 0.09
Liver	0.60 ± 0.18	0.78 ± 0.26	0.18 ± 0.10
Kidneys	0.014 ± 0.002	0.029 ± 0.008	0.007 ± 0.003
Blood	0.126 ± 0.051	0.203 ± 0.046	0.052 ± 0.022
Lungs	0.0094 ± 0.0026	0.0160 ± 0.0025	0.0062 ± 0.0026
Heart	0.0042 ± 0.0016	0.0060 ± 0.0015	0.0032 ± 0.0007
Pancreatic gland	0.0079 ± 0.0015	0.0120 ± 0.0052	0.0039 ± 0.0013
Spleen	0.054 ± 0.020	0.059 ± 0.029	0.010 ± 0.004
Gonads	0.016 ± 0.003	0.033 ± 0.007	0.010 ± 0.004
Brain	0.0029 ± 0.0010	0.0123 ± 0.0023	0.0053 ± 0.0017
Urine	0.012 ± 0.002	0.032 ± 0.009	0.048 ± 0.037

b. Silver nanoparticles labelled by ^{110m}Ag radioisotope

The measurements of the ^{110m}Ag tracer in the organs of rats after administration of labelled silver NPs showed that >98% of the activity is located in the gastrointestinal tract and then excreted with faeces. The total NP absorption from the gastrointestinal tract throughout the experiment did not exceed 2% of the administered dose for all animals. Nevertheless, owing to the high specific activity of the ^{110m}Ag-labelled NPs, the NP distribution among the organs and tissues was estimated by γ-spectrometric analysis. It follows from the data presented in Table 4 that silver NPs are mainly accumulated in the liver; the overall tracer activity in the liver is similar in the order of magnitude to the overall activity in all other organs and tissues.

In the order of decreasing ^{110m}Ag, the next are peripheral blood, spleen and gonads. The tracer accumulation in the heart did not exceed 3% – 6% of the content in the blood and may be related to the amount remaining in the coronary vessels. The total content of ^{110m}Ag NPs in the kidneys, lungs and pancreatic gland is also insignificant. Note the following: if the data are expressed in the units of specific NP content in the sample rather than in the units of total NP content in the organs (Fig. 13), then the second highest NP concentration after the liver was found in the spleen.

Note the low level of NP accumulation in the brain. This can also be attributed, to an extent, to the retention of the NPs in the brain blood vessels. However, the maximum ^{110m}Ag NP concentration in the brain (attained ~48 h after administration) does not coincide in time with the blood maximum, which is observed in the range of 24 – 48 h (see Fig. 13). Obviously, some silver NPs penetrate the blood–brain barrier. However, verification of these data and accurate quantitative evaluation require additional research.

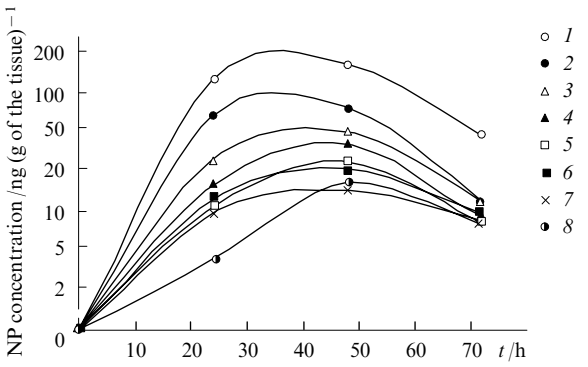


Figure 13. Concentration of ^{110m}Ag-labelled silver NPs in the body of rats *vs.* time after intragastric administration through enteral tube.
Organ: (*1*) liver, (*2*) spleen, (*3*) blood, (*4*) kidney, (*5*) lungs, (*6*) gonads, (*7*) heart, (*8*) brain.

c. Gold nanoparticles labelled by ^{198}Au radioisotope

The results of estimation of the absorption and distribution among organs and tissues for ^{198}Au-labelled gold NPs are summarized in Table 5 and in Fig. 14. Like silver and titanium dioxide NPs, gold NPs show very low absorption upon intragastric administration. The total faecal and gastrointestinal content of the tracer 24 and 48 h after administration exceeds 95%, and after 72 h, it did not differ from 100% to within the error of γ-spectrometric analysis, *i.e.*, the main bulk of gold NPs is excreted with the faeces. The urine excretion is very low, being <0.02% of the administered amount during the first 24 h.

However, the biokinetics and organotropism of gold NPs are largely different from those of silver NPs, despite the fact that both these metals are chemically inert under physiological conditions. The most pronounced accumulation of gold NPs was found in kidneys. In the order of decreasing tracer activity, this is followed by the blood, liver and spleen. The tracer accumulation in other organs is rather low — it does not exceed 10^{-2}% of the administered dose. The residual amount of labelled gold NPs in the bones is apparently much lower than that of silver NPs.

Table 5. Distribution of ^{198}Au in the body of rats at various time intervals after intragastric administration of ^{198}Au-labelled gold NPs (in percent of the administered dose, $M \pm m$).

Biological specimen	Time after administration /h		
	24	48	72
GIT	64.2 ± 6.8	5.93 ± 3.42	0.199 ± 0.064
Faeces	31.1 ± 11.0	89.1 ± 8.1	100 ± 3
Carcass	0.145 ± 0.061	0.0078 ± 0.0068	0.0054 ± 0.0045
Liver	0.018 ± 0.003	0.045 ± 0.036	0.0039 ± 0.0013
Kidneys	0.166 ± 0.029	0.114 ± 0.091	0.069 ± 0.014
Blood	0.037 ± 0.003	0.035 ± 0.018	0.0042 ± 0.0021
Lungs	0.0073 ± 0.0012	0.0040 ± 0.0031	0.0052 ± 0.0029
Heart	0.0023 ± 0.0006	0.0027 ± 0.0012	0.0016 ± 0.0007
Pancreatic gland	0.0033 ± 0.0011	0.0018 ± 0.0012	0.0017 ± 0.0014
Spleen	0.0095 ± 0.0024	0.0088 ± 0.0070	0.0090 ± 0.0061
Gonads	0.0086 ± 0.0028	0.0042 ± 0.0031	0.0028 ± 0.0012
Brain	0.00038 ± 0.00017	0.00070 ± 0.00026	0.00025 ± 0.00012
Urine	0.012 ± 0.002	see [a]	see [a]

[a] No measurements were performed.

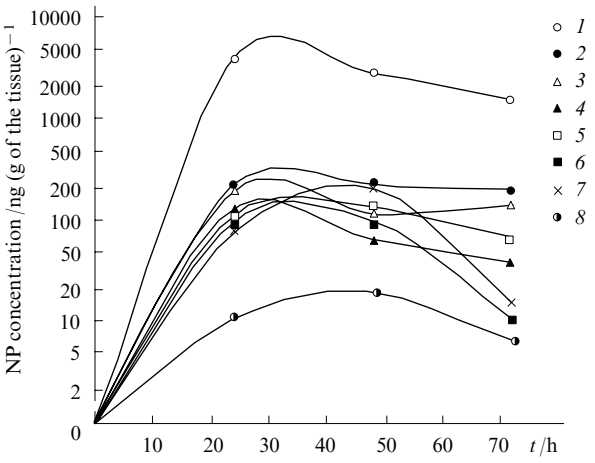


Figure 14. Concentration of ^{198}Au-labelled gold NPs in the body of rats *vs.* time after intragastric administration through enteral tube. Organ: (*1*) kidneys, (*2*) spleen, (*3*) lungs, (*4*) gonads, (*5*) heart, (*6*) blood, (*7*) liver, (*8*) brain.

Note that the minor amounts of gold NPs revealed in the pancreatic gland, lungs and gonads show a sort of 'conservation', *i.e.*, their amount in these organs does not tend to decrease (to within the determination error) after 72 h as compared with the amount found after 48 h. The time variation curves for the specific content of gold NPs per unit weight of the organ are shown in Fig. 14. It can be seen that the highest concentration of these NPs is found in kidneys, and it is an order of magnitude higher than the second highest concentration found in the spleen. In the brain, the total amount and the concentration of NPs 24 h after administration are an order of magnitude lower than those in the blood. Thus, it cannot be ruled out that in an early stage of the experiment, the whole or almost the whole amount of ^{198}Au detected in the region of brain may actually be due to the NPs present in the blood vessel lumen of the brain. However, after 72 h, the NP concentrations in the blood and in the brain differ less than twofold. Moreover, as in the case of silver NPs, the highest content of gold NPs in the brain is reached later (after 48 h) than in the blood (in the range from 24 to 48 h). This suggests that some minor portion of gold NPs can penetrate the blood–brain barrier. However, the degree of penetration cannot be quantitatively determined based on the experimental data.

The reasons for the considerable difference between the organotropisms of silver and gold NPs are obscure. The surface of the NPs administered into animals bears a loosely bound adsorption layer of stabilizer molecules (polyvinylpyrrolidone and citric acid, respectively); as NPs enter the body, this layer is apparently replaced by a layer (crown) of the animal body proteins.[159, 160] Presumably, the abilities of silver and gold NPs to bind various blood plasma proteins are different, which accounts for different degrees of their retention by the cell receptors of liver and kidneys. However, this assumption requires experimental verification.

d. Selenium nanoparticles labelled by the ^{75}Se radioisotope

As follows from the data summarized in Table 6 and in Fig. 15, the distribution of ^{75}Se-labelled selenium NPs in the rat body after the intragastric administration differs substantially from the distribution of other studied NPs. Note a rather high degree of absorption of selenium NPs during the first 24 h after administration; subsequently $\sim$40% of the selenium present in the NPs is excreted with the faeces and $\sim$55% is excreted with the urine. The highest ^{75}Se concentration was detected in kidneys; large amounts of selenium are accumulated in the blood and liver. Considerable amounts of the tracer (4%–5%) were found also in the carcass. In all of the studied organs, except for brain, the maximum tracer concentration is attained between 24 and 48 h after administration, and by 72 h of the experiment, some 'conservation' of the

Table 6. Distribution of ^{75}Se in the body of rats at various time intervals after intragastric administration of ^{75}Se-labelled selenium NPs (in percent of the administered dose, $M \pm m$).

Biological specimen	Time after administration h		
	24	48	72
GIT	31.6 ± 3.8	5.20 ± 1.71	1.23 ± 0.38
Faeces	4.78 ± 1.71	33.5 ± 3.3	36.7 ± 1.7
Carcass	5.20 ± 0.68	4.30 ± 0.43	4.24 ± 1.15
Liver	3.34 ± 0.17	2.55 ± 0.32	2.61 ± 0.25
Kidneys	1.50 ± 0.08	1.31 ± 0.15	1.21 ± 0.13
Blood	4.11 ± 0.17	3.24 ± 0.39	3.71 ± 0.47
Lungs	0.211 ± 0.013	0.206 ± 0.015	0.187 ± 0.015
Heart	0.093 ± 0.008	0.077 ± 0.008	0.063 ± 0.022
Pancreatic gland	0.106 ± 0.012	0.059 ± 0.010	0.088 ± 0.003
Spleen	0.272 ± 0.044	0.220 ± 0.029	0.222 ± 0.025
Gonads	0.275 ± 0.030	0.268 ± 0.013	0.293 ± 0.017
Brain	0.035 ± 0.003	0.050 ± 0.015	0.032 ± 0.001
Urine	50.7 ± 3.0	54.8 ± 2.0	57.1 ± 2.3

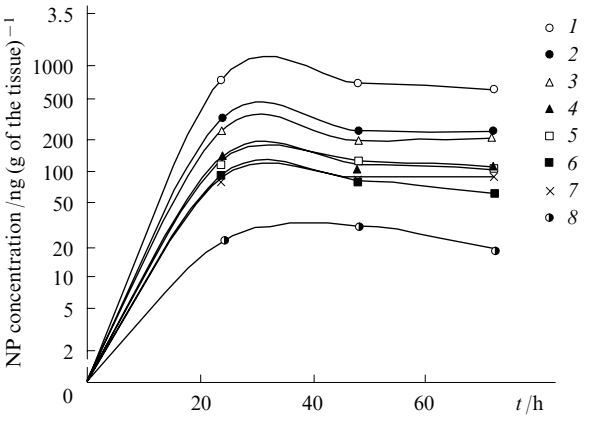


Figure 15. Concentration of ^{75}Se-labelled NPs and the possible products of their metabolism in the body of rats *vs*. time after intragastric administration.
Organ: (*1*) kidneys, (*2*) liver, (*3*) blood, (*4*) spleen, (*5*) lungs, (*6*) heart, (*7*) gonads, (*8*) brain.

content of exogenous labelled selenium takes place, or its amount even increases (as it was found for blood).

The smallest amount of ^{75}Se was found in the brain (not higher than 1% – 2% of the blood level). The most pronounced decrease in the specific activity in the brain occurred by 72 h after ^{75}Se administration. This may imply retention of the tracer activity in the residual blood of brain capillaries and the lack of evidence for penetration of considerable amounts of nanoparticles or the products of their biotransformations through the blood – brain barrier.

These results suggest that unlike silver and gold NPs, selenium particles are considerably biotransformed and metabolized in the body, *i.e*., selenium is incorporated into the metabolic process. The main bulk is excreted with urine, and only a slight amount is deposited in the liver and kidneys. This fact comes as no surprise as most of the possible sites of selenium incorporation into protein molecules are saturated with selenium that arrived into the animal body with food. In eukaryotes, the co-translational incorporation of selenium into proteins as selenocysteine is known to be sharply intensified in the case of selenium deficiency and, conversely, to be retarded when selenium is present in normal or excessive amount. The greater part of selenium that was not included into biosynthetic processes is methylated and excreted with urine,[161] which is apparently the case in our experiments.

e. Zinc nanoparticles labelled by the ^{65}Zn radioisotope

The results of determination of ^{65}Zn in the urine and faeces and the absorption, retention and effective retention factors of zinc from the ^{65}Zn-labelled specimen are summarized in Table 7. The data attest to very high bioavailability of zinc when present in zinc oxide NPs. The overall activity of the tracer that has not been absorbed in the intestines is only ~20%. Hence, in view of the characteristic transit time of the intestine content, which is ~24 h for rats, not less than 80% of the amount of the introduced tracer is absorbed in the intestines. In reality, the absorption in the intestines can be even higher taking into account the fact that some of the zinc oxide NPs absorbed during the first 24 h has time to be metabolized in the body and be incorporated in proteins, some of which can get into the intestines, for example, as a part of pancreatic juice or bile.

Table 7. Characteristics of zinc bioavailability in rats upon administration of ^{65}Zn-labelled ZnO nanoparticles.

Characteristics	$M \pm m$
Faecal excretion of ^{65}Zn (% of the administered dose)	20.01 ± 4.65
Urine excretion of ^{65}Zn (% of the administered dose)	0.60 ± 0.24
Assimilability characteristics:	
absorption factor (%)	80.00 ± 4,65
retention factor (%)	79.39 ± 4.61
effective retention factor (%)	99.25 ± 0.28

The zinc absorbed as NPs is effectively retained in the body for 24 h, as indicated by low urine excretion of the tracer. Therefore, the tracer retention factor differs little from the absorption factor. The absorbed zinc oxide NPs are utilized almost completely in the body, as indicated by the effective retention factor exceeding 99%.

The statement of the high bioavailability of zinc in the form of zinc oxide NPs is even more significant because the study was performed for animals supplied with enough zinc in the diet. Under conditions of zinc deficiency, the intestinal absorption and retention may be even higher.

As follows from the data presented in Table 8, zinc introduced in the gastrointestinal tract of rats as NPs, after penetration into the body, is distributed in different ways in the internal organs. The greatest amount of the tracer was detected in the liver and kidneys of the animals; in the order of decreasing amount, this is followed by spleen, pancreatic gland, gonads, lungs,

Table 8. Distribution of ^{65}Zn in the body of rats at various time intervals after intragastric administration of ^{65}Zn-labelled zinc oxide NPs (in percent of the administered dose, $M \pm m$).

Biological specimen	Time after administration /h			
	4	24	72	120
Blood	0.126 ± 0.025	0.244 ± 0.053	0.475 ± 0.09	0.171 ± 0.020
Brain	0.021 ± 0.005	0.036 ± 0.013	0.064 ± 0.003	0.047 ± 0.004
Heart	0.061 ± 0.016	0.112 ± 0.042	0.166 ± 0.078	0.049 ± 0.01
Lungs	0.076 ± 0.012	0.148 ± 0.018	0.189 ± 0.036	0.068 ± 0.018
Seminal glands	0.078 ± 0.012	0.180 ± 0.025	0.196 ± 0.029	0.072 ± 0.011
Pancreatic gland	0.177 ± 0.037	0.214 ± 0.082	0.227 ± 0.037	0.0290 ± 0.080
Kidneys	0.376 ± 0.094	0.428 ± 0.101	0.536 ± 0.065	0.116 ± 0.007
Liver	2.502 ± 0.489	3.878 ± 0.558	3.977 ± 0.789	1.16 ± 0.115
Spleen	0.199 ± 0.072	0.256 ± 0.045	0.354 ± 0.093	0.105 ± 0.029

[a] The amount of zinc nanoparticles administered into the gastrointestinal tract is 1 mg per rat, which corresponds to the 50 kBq activity of ^{65}Zn.

heart and brain. Note relatively low zinc uptake in the blood and brain, despite the considerable number of Zn-containing proteins in the tissues of these organs. The maximum uptake of the tracer in all organs was observed 72 h after administration. By the 120th hour of observation, the tracer activity decreased in all of the organs, which is consistent with the known fast turnover of Zn-containing proteins (many of which are enzymes) and the absence of pronounced zinc deposition under sufficient supply.

The greatest amount of ^{65}Zn is deposited in the musculoskeletal carcass of the animals. As in the internal organs, the maximum tracer inclusion in the frame was noted 72 h after the beginning of the experiment, while after 120 h excretion of ^{65}Zn started.

Analysis of the individual distribution profiles of ^{65}Zn among the biosubstrates of rats obtained in 72- and 120-h experiments [13, 155] showed that most of zinc introduced with the specimen is detected in the frame (27% – 40%) and is excreted with the faeces (28% – 51%). A considerable amount of the tracer is detected after 72 h in the gastrointestinal tract (16% – 40%) and liver (3% – 5%). The amount of tracer retained in other organs is negligibly low. After 72 h, the main bulk of ^{65}Zn (82% – 84%) is excreted with the faeces, and only 10% – 13% is retained in the frame. Note very low levels of zinc excretion with urine observed in all experiments.

Thus, the studies by the radioactive tracer method identified several types of behaviour of inorganic NPs entering the gastrointestinal tract. Apparently, titanium dioxide NPs tend to show extremely low degree of absorption from the gastrointestinal tract and nearly 100% faecal excretion. Conversely, small but reliably detectable amounts of silver and gold NPs penetrate through the intestinal walls and are accumulated in organs and tissues, the organotropism profiles for these two types of NPs being substantially different. Finally, the selenium and zinc oxide NPs show fairly high degree of absorption, which is presumably accompanied by biotransformation and urine and faecal excretion, respectively. The results attest to good prospects of using radioactive tracers for studying absorption, biodistribution and excretion of engineered NPs, in particular, for elucidating the reasons of different organotropism of metal NPs and the possible routes and mechanisms of their assimilation.

* * *

In conclusion, it should be noted that integrated physiologo-biochemical and toxicologo-hygienic assessment of adsorption, biodistribution and bioaccumulation of nanoparticles and nanomaterials in the body cannot currently be based on any single known method of their analysis in heterogeneous and multicomponent systems. An integrated approach is required including the use of electron microscopy, chemical analysis and model *in vivo* experiments using labelled nanoparticles.

The authors are sincerely grateful to S M Pridvorova, T A Platonova, O V Morozova, A I Yaropolov (A N Bakh Institute of Biochemistry of the RAS), K V Kotenko, V S Kalistratova, R G Nisimova, V Yu Soloviev (A I Burnyazyan Federal Centre of Medical Biophysics, Federal Medicobiological Agency), P G.Kuzmin, G A Shafeev (Wave Research Centre of the A M Prokhorov General Physics Institute of the RAS), A G Volkovich, T I Kuznetsova, S T Latushkin, N S Marchenkov, V N Unezev (Research Centre Kurchatov Institute), L S Vasilevskaya, R V Raspopov, E A Arianova, A A Shumakova (Scientific Research Institute of Nutrition, Russian Academy of Medical Sciences) for providing experimental data and illustrative material.

This work was performed with the support of the Ministry of Education and Science of the Russian Federation (Federal Target Programme 'Development of the Infrastructure of Nanoindustry in the Russian Federation for 2008 – 2011', state contracts No. 16.648.12.3001 and No. 01.648.12.3022).

References

1. P J Borm, D Robbins, S Haubold, T Kuhlbusch, H Fissan, K Donaldson, R Schins, V Stone, W Kreyling, J Lademann, J Krutmann, D Warheit, E Oberdlrster *Part. Fibre Toxicol.* **3** 1 (2006)
2. G Oberdörster, A Maynard, K Donaldson, V Castranova, J Fitzpatrick, K Ausman, J Carter, B Karn, W Kreyling, D Lai, S Olin, N Monteiro-Riviere, D Warheit, H Yang *Part. Fibre Toxicol.* **2** 8 (2005)
3. G Oberdörster, E Oberdörster, J Oberdörster *Environ. Health Persp.* **113** 823 (2005)
4. S A Khotimchenko, I V Gmoshinski, V A Tutel'yan *Gigiena Sanitar.* (5) 7 (2009)
5. M V Alfimov, V F Razumov *Ros. Nanotekhnol.* **2** (1 – 2) 12 (2007) [a]
6. Q Chaudhry, M Scotter, J Blackburn, B Ross, A Boxall, L Castle, R Aitken, R Watkins *Food Addit. Contam.* **25** 241 (2008)
7. V M Vernikov, E A Arianova, I V Gmoshinski, S A Khotimchenko, V A Tutel'yan *Vopr. Pitan.* **78** (2) 4 (2009)
8. V V Nevzorova, I V Gmoshinski, S A Khotimchenko *Vop. Pitan.* **78** (4) 54 (2009)
9. K I Popov, A N Filippov, S A Khurshudyan *Ros. Khim. Zh.* **53** (2) 86 (2009) [b]
10. In *Down on the Farm: the Impact of Nano-Scale Technologies on Food and Agriculture* (Ottawa: ETC Group Report, 2004) p. 1
11. J Zhang, X Wang, T Xu *Toxicol. Sci.* **101** 22 (2008)
12. F Rohner, F O Ernst, M Arnold, M Hilbe, R Biebinger, F Ehrensperger, S E Pratsinis, W Langhans, R F Hurrell, M B Zimmermann *J. Nutr.* **137** 614 (2007)
13. R V Raspopov, Yu P Buzulukov, N S Marchenkov, V Yu Solov'ev, V F Demin, V S Kalistratova, I V Gmoshinski, S A Khotimchenko *Vopr. Pitan.* **79** (6) 14 (2010)
14. R V Raspopov, E A Arianova, E N Trushina, G Yu Mal'tsev, P G Kuz'min, G A Shafeev , S M Pridvorova, I V Gmoshinski, S A Khotimchenko *Vopr. Pitan.* **80** (4) 36 (2011)
15. R V Raspopov, E N Trushina, I V Gmoshinski, S A Khotimchenko *Vopr. Pitan.* **80** (3) 25 (2011)
16. I V Gmoshinski, V V Smirnova, S A Khotimchenko *Ros. Nanotekhnol.* **5** (9 – 10) 6 (2010) [a]
17. V M Vernikov, I V Gmoshinski, S A Khotimchenko *Vopr. Pitan.* **78** (6) 13 (2009)
18. L B Piotrovskii, O I Kiselev *Fullereny v Biologii* (Fullerenes in Biology) (St Petersburg: Rostok, 2006)
19. J M Balbus, A D Maynard, V L Colvin, V Castranova, G P Daston, R A Denison, K L Dreher, P L Goering, A M Goldberg, K M Kulinowski, N A Monteiro-Riviere, G Oberdörster, G S Omenn, K E Pinkerton, K S Ramos, K M Rest, J B Sass, E K Silbergeld, B A Wong *Environ. Health Persp.* **115** 1654 (2007)
20. H Bouwmeester, S Dekkers, M Y Noordam, W I Hagens, A S Bulder, C de Heer, S E C G ten Voorde, S W Wijnhoven, H J Marvin, A J Sips *Regul. Toxicol. Pharmacol.* **53** 52 (2009)
21. G G Onishchenko, V A Tutel'yan *Vopr. Pitan.* **76** (6) 4 (2007)
22. G G Onishchenko, A I Archakov, V V Bessonov, B G Bokit'ko, A L Gintsburg, I V Gmoshinski, A I Grigor'ev, N F Izmerov, M P Kirpichnikov, B S Naroditskii, V I Pokrovskii, A I Potapov, Yu A Rakhmanin, V A Tutel'yan, S A Khotimchenko, K V Shaitan, S A Sheveleva *Gigiena Sanitar.* (6) 3 (2007)
23. *Razvitie Metodicheskoi Sostavlyayushchei Infrastruktury Nanoindustrii. Federal'naya Tselevaya Programma 'Razvitie Infrastruktury Nanoindustrii v Rossiiskoi Federatsii na 2008 – 2011 Gody' (Sbornik Informatsionno-Analiticheskikh Materialov)* [Development of Methodological Component of the Infrastructure of Nanoindustry. Federal Target Programme 'Development of the Infrastructure of Nanoindustry in the Russian Federation for 2008 – 2011' (Collection of Information and Analytical Materials)] (Moscow: The Ministry of Education and Science of the Russian Federation, 2011) Vol. 3
24. K Tiede, A B Boxall, S P Tear, J Lewis, H David, M Hassellöv *Food Addit.Contam.* **25** 795 (2008)
25. A D Maynard *Philos. Trans. R. Soc. London, A* **358** 2593 (2000)
26. D Mavrocordatos, D Perret, G G Leppard, in *Environmental Colloids and Particles: Behaviour, Structure and Characterization* (Chichester: Wiley, 2007) p. 345
27. M Hassellöv, J W Readman, J F Ranville, K Tiede *Ecotoxicology* **17** 344 (2008)
28. K I Popov, I V Gmoshinski, A N Filippov, A V Zherdev, S A Khotimchenko, V A Tutel'yan *Pishchevye Nanotekhnologii: Perspektivy i Problemy* (Food Nanotechnologies: Perspectives and Problems) (Moscow: Moscow State University of Food Production 2010
29. K Tiede, M Hassellöv, E Breitbarth, Q Chaudhry, A B Boxall *J. Chromatogr., A* **1216** 503 (2008)
30. B Nowack, T D Bucheli *Environ. Pollut.* **150** 5 (2007)
31. J D Fortner, D Y Lyon, C M Sayes, A M Boyd, J C Falkner, E M Hotze, L B Alemany, Y J Tao, W Guo, K D Ausman, V L Colvin, J B Hughes *Environ. Sci. Technol.* **39** 4307 (2005)
32. T Phenrat, S Naleh, K Sirk, R D Tilton, G V Lowry *Environ. Sci. Technol.* **41** 284 (2007)
33. J G Teeguarden, P M Hinderliter, G Orr, B D Thrall, J G Pounds *Toxicol. Sci.* **95** 300 (2007)
34. H Hyung, J D Fortner, J B Hughes, J H Kim *Environ. Sci. Technol.* **41** 179 (2007)
35. S F Hansen, B H Larsen, S I Olsen, A Baun *Nanotoxicology* **1** 243 (2007)
36. O D Gendrikson, I V Safenkova, A V Zherdev, B B Dzantiev, V O Popov *Biofizika* **56** 965 (2011) [c]
37. M Takahashi, Kinafuku, T Miyagi, H Oku, K Wada, T Imura, D Kitamoto *J. Oleo Sci.* **56** 35 (2007)
38. V Prasad, D Semwogerere, E R Weeks *J. Phys: Condens. Matter* **19** 113102 (2007)
39. F Li, X Zhou, J Zhu, J Ma, X Huang, S T Wong *BMC Biotechnology* **7** 1 (2007)
40. P R Buseck, K Adachi, in *Abstract of the 42nd Western Regional Meeting of American Chemical Societ. Washington, 2008* p. 180
41. D Mavrocordatos, W Pronk, M Boller *Water Sci. Technol.* **50** 9 (2004)
42. A Gojova, B Guo, R S Kota, J C Rutledge, I M Kennedy, A I Barakat *Environ. Health Persp.* **115** 403 (2007)
43. P L Apopa, Y Qian, R Shao, N L Guo, D Schwegler-Berry, M Pacurari, D Porter, X Shi, V Vallyathan, V Castranova, D C Flynn *Part. Fibre Toxicol.* **6** 1 (2009)
44. K Yamamoto, M Makino, in *International Symposium on the Risk Assessment of Manufactured Nanomaterials (Abstract Book), Tokyo, 2008* p. 25
45. A E Porter, M Gass, K Muller, J N Skepper, P Midgley, M Welland *Environ. Sci. Technol.* **41** 3012 (2007)
46. J Y Liu *J. Electron. Microsc.* **54** 251 (2005)

47. S Utsunomiya, R C Ewing *Environ. Sci. Technol.* **37** 786 (2003)
48. J D Richman, K J Livi, A S Geyh *J. Aerosol Sci.* **42** 408 (2011)
49. J Thieme, I McNulty, S Vogt, D Paterson *Environ. Sci. Technol.* **41** 6885 (2007)
50. J T Nurmi, P G Tratnyek, V Sarathy, D R Baer, J E Amonette, K Pecher, C Wang, J C Linehan, D W Matson, R L Penn, M D Driessen *Environ. Sci. Technol.* **39** 1221 (2005)
51. C Y Wang, C Bottcher, D W Bahnemann, J K Dohrmann *J. Nanopart. Res.* **6** 119 (2004)
52. G G Leppard, D Mavrocordatos, D Perret *Water Sci. Technol.* **50** 1 (2004)
53. F J Doucet, J R Lead, L Maguire, E P Achterberg, G E Millward *J. Environ. Monit.* **7** 115 (2005)
54. P S Redwood, J R Lead, R M Harrison, I P Jones, S Stoll *Environ. Sci. Technol.* **39** 1962 (2005)
55. A Bogner, G Thollet, D Basset, P H Jouneau, C Gauthier *Ultramicroscopy* **104** 290 (2005)
56. S Thiberge, O Zik, E Moses *Rev. Sci. Instrum.* **75** 2280 (2004)
57. W Timp, N Watson, A Sabban, O Zik, P Matsudaira *BioTechniques* **41** 295 (2007)
58. S Thiberge, A Nechushtan, D Sprinzak, O Gileadi, V Behar, O Zik, Y Chowers, S Michaeli, J Schlessinger, E Moses *Proc. Natl. Acad. Sci., USA* **101** 3346 (2004)
59. C Mühlfeld, B Rothen-Rutishauser, D Vanhecke, F Blank, P Gehr, M Ochs *Part. Fibre Toxicol.* **4** 11 (2007)
60. E Balnois, G Papastavrou, I Wilkinson, in *Environmental Colloids and Particles: Behaviour, Structure and Characterization* (Chichester: Wiley, 2007) p. 405
61. L Zhu, P Attard, C Neto *Langmuir* **27** 6712 (2011)
62. A Shluger, T Trevethan *Nature (London)* **446** 34 (2007)
63. Y Sugimoto, P Pou, M Abe, P Jelinek, R Pérez, S Morita, O Custance *Nature (London)* **446** 64 (2007)
64. I V Safenkova, A V Zherdev, B B Dzantiev *J. Immunol. Methods* **357** 17 (2010)
65. J R Lead, D Muirhead, C T Gibson *Environ. Sci. Technol.* **39** 6930 (2005)
66. E Balnois, K J Wilkinson *Colloids Surf., A* **207** 229(2002)
67. H S Yang, Y F Wang, S J Lai, H An, Y Li, F Chen *J. Food Sci.* **72** 65 (2007)
68. N S Wigginton, K M Rosso, B H Lower, L Shi, M F Hochella Jr *Geochim. Cosmochim. Acta* **71** 543 (2007)
69. S Katano, K Toma, M Toma, K Tamada, Y Uehara *Phys. Chem. Chem. Phys.* **12** 14749 (2010)
70. A Helfrich, W Bruchert, J Bettmer *J. Anal. Atom. Spectrom.* **21** 431 (2006)
71. Y Song, M L Heien, V Jimenez, R M Wightman, R W Murray *Anal. Chem.* **76** 4911 (2004)
72. T Cedervall, I Lynch, S Lindman, T Berggård, E Thulin, H Nilsson, K A Dawson, S Linse *Proc. Natl. Acad. Sci. USA* **104** 2050 (2007)
73. X Y Huang, R S McLeanand, M Zheng *Anal. Chem.* **77** 6225 (2005)
74. K M Krueger, A M Al-Somali, J C Falkner, V L Colvin *Anal. Chem.* **77** 3211 (2005)
75. K J Ziegler, D J Schmidt, U Rauwald, K N Shah, E L Flor, R H Hauge, R E Smalley *Nano Lett.* **5** 2355 (2005)
76. J R Lead, K J Wilkinson *Environ. Chem.* **3** 159 (2006)
77. B Porsch, A Welinder, A Korner, B Wittgren *J. Chromatogr., A* **1068** 249 (2005)
78. M T Blom, E Chmela, R E Oosterbroek, R Tijssen, A van den Berg *Anal. Chem.* **75** 6761 (2003)
79. E Chmela, R Tijssen, M T Blom, H J Gardeniers, A van den Berg *Anal. Chem.* **74** 3470 (2002)
80. A Williams, E Varela, E Meehan, K Tribe *Int. J. Pharm.* **242** 295 (2002)
81. B A Yegin, A Lamprecht *Int. J. Pharm.* **320** 165 (2006)
82. X R Xia, N A Monteiro-Riviere, J E Riviere *J. Chromatogr., A* **1129** 216 (2006)
83. T M Benn, B F Pycke, P Herckes, P Westerhoff, R U Halden *Anal. Bioanal. Chem.* **399** 1631 (2011)
84. F Moussa, M Pressac, E Genin, S Roux, F Trivin, A Rassat, R Céolin, H Szwarc *J. Chromatogr., B* **696** 153 (1997)
85. G L Baker, A Gupta, M L Clark, B R Valenzuela, L M Staska, S J Harbo, J T Pierce, J A Dill *Toxicol. Sci.* **101** 122 (2008)
86. P K Zarzycki, H Ohta, F B Harasimiuk, K Jinno *Anal. Sci.* **23** 1391 (2007)
87. M Hassellöv , F von der Kammer, R Beckett, in *Environmental Colloids and Particles: Behaviour, Structure and Characterization, Chichester, 2007* p. 223
88. M Baalousha, F von der Kammer, M Motelica-Heino, P Le Coustumer *J. Chromatogr., A* **1093** 156 (2005)
89. F von der Kammer, M Baborowski, K Friese *Anal. Chim. Acta* **552** 166 (2005)
90. M Baalousha, J R Lead *Environ. Sci. Technol.* **41** 1111 (2007)
91. M Graff, A B Frazier *IEEE Trans. Nanotechnol.* **5** 8 (2006)
92. H Q Peng, N T Alvarez, C Kittrell, R H Hauge, H K Schmidt *J. Am. Chem. Soc.* **128** 8396 (2006)
93. L Calzolai, D Gilliland, C P García, F Rossi *J. Chromatogr., A* **1218** 4234 (2011)
94. M Baalousha, B Stolpe, J R Lead *J. Chromatogr., A* **1218** 4078 (2011)
95. A Bootz, V Vogel, D Schubert, J Kreuter *Eur. J. Pharm. Biopharm.* **157** 369 (2004)
96. L J Gimbert, P M Haygarth, R Beckett, P J Worsfold *Environ. Sci. Technol.* **39** 1731 (2005)
97. F J Doucet, L Maguire, J R Lead *Talanta* **67** 144 (2005)
98. R X Liu, J R Lead *Anal. Chem.* **78** 8105 (2006)
99. R X Liu, J R Lead, A Baker *Chemosphere* **68** 1304 (2007)
100. F J Doucet, L Maguire, J R Lead *Anal. Chim. Acta* **522** 59 (2004)
101. M V Tikhonova, L V Tsiro, L N Andreeva, S Ya Aleksandrova, F G Unger *Perspekt. Mater.* **4** 92 (2007)
102. H Nomura, K Katayama *Anal. Sci.* **24** 459 (2008)
103. J H Lee, Y Roh, H G Hur *J. Microbiol. Biotechnol.* **18** 1572 (2008)
104. S Takegami, K Kitamura, H Kawada, Y Matsumoto, T Kitade, H Ishida, C Nagata *Chem. Pharm. Bull.* **56** 1097 (2008)
105. R C Murdock, L Braydich-Stolle, A M Schrand, J J Schlager, S M Hussain *Toxicol. Sci.* **101** 239 (2008)
106. M S Diallo, C J Glinka, W A Goddard, J H Johnson *J. Nanopart. Res.* **7** 435 (2005)
107. S Keren, C Zavaleta, Z Cheng, A de la Zerda, O Gheysens, S S Gambhir *Proc. Natl. Acad. Sci. USA* **105** 5844 (2008)
108. D A Watson, L O Brown, D F Gaskill, M Naivar, S W Graves, S K Doorn, J P Nolan *Cytometry, A* **73** 119 (2008)
109. M Hu, J Chen, M Marquez, Y Xia, G V Hartland *J. Phys. Chem. C* **111** 12558 (2007)
110. R S Carter, S J Harley, P P Power, M P Augustine *Chem. Mater.* **17** 2932 (2005)

111. M Valentini, A Vaccaro, A Rehor, A Napoli, J A Hubbell, N Tirelli *J. Am. Chem. Soc.* **126** 2143 (2004)
112. H Kato, K Takahashi, T Saito *Chem. Phys. Lett.* **463** 150 (2008)
113. J R Lead, A De Momi, G Goula, A Baker *Anal. Chem.* **78** 3609 (2006)
114. Y Cai, W P Peng, H C Chang *Anal. Chem.* **75** 1805 (2003)
115. W P Peng, Y Cai, Y T Lee, H C Chang *Int. J. Mass Spectrom.* **229** 67 (2003)
116. Z-J Zhu, P S Ghosh, O M Miranda, R W Vachet, V M Rotello *J. Am. Chem. Soc.* **130** 14139 (2008)
117. E Fabian, R Landsiedel, L Ma-Hock, K Wiench, W Wohlleben, B van Ravenzwaay *Arch. Toxicol.* **82** 151 (2008)
118. K Sigubayashi, H Todo, E Kimura *J. Toxicol. Sci.* **33** 293 (2008)
119. C Janzen, H Kleinwechter, J Knipping, H Wiggers, P Rothet *J. Aerosol. Sci.* **33** 833 (2002)
120. D Lee, K Park, M R Zachariah *Aerosol. Sci. Technol.* **39** 162 (2005)
121. T Ito, L Sun, R M Crooks *Anal. Chem.* **75** 2399 (2003)
122. G Suresh, K Manjunath, V Venkateswarlu, V Satyanarayana *AAPS Pharm. Sci. Technol.* **8** 1 (2007)
123. P Bihari, M Vippola, S Schultes, M Praetner, A G Khandoga, C A Reichel, C Coester, T Tuomi, M Rehberg, F Krombach *Part. Fibre Toxicol.* **5** 1 (2008)
124. H Reiber, T Köller, T Palberg, F Carrique, E Ruiz Reina, R Piazza *J. Colloid Interface Sci.* **309** 315 (2007)
125. T Pellegrino, R A Sperling, A P Alivisatos, W J Parak *J. Biomed. Biotechnol.* 26796 (2007)
126. K H Lin, T C Chu, F K Liu *J. Chromatogr., A* **1161** 314 (2007)
127. P Schmitt-Kopplin, J Junkers *J. Chromatogr., A* **998** 1 (2003)
128. S C Lee, R Parthasarathy, T D Duffin, K Botwin, J Zobel, T Beck, G Lange, D Kunneman, R Janssen, E Rowold *Biomed. Microdev.* **3** 53 (2001)
129. B X Chen, S R Wilson, M Das, D J Coughlin, B F Erlanger *Proc. Natl. Acad. Sci. USA,* **95** 10809 (1998)
130. B C Braden, F A Goldbaum, B X Chen, A N Kirschner, S R Wilson, B F Erlanger *Proc. Natl. Acad. Sci. USA* **97** 12193 (2000)
131. O D Hendrickson, N S Fedyunina, A A Martianov, A V Zherdev, B B Dzantiev *J. Nanopart. Res.* **13** 3713 (2011)
132. O D Hendrickson, N S Fedyunina, A V Zherdev, O N Solopova, P G Sveshnikov, B B Dzantiev *Analyst* **137** 98 (2012)
133. D Canevet, M Gallego, H Isla, A de Juan, E M Pérez, N Martín *J. Am. Chem. Soc.* **133** 3184 (2011)
134. G Gil-Ramírez, S D Karlen, A Shundo, K Porfyrakis, Y Ito, G A Briggs, J J Morton, H L Anderson *Org. Lett.* **12** 3544 (2010)
135. K W Powers, S C Brown, V B Krishna, S C Wasdo, B M Moudgil, S M Roberts *Toxicol. Sci.* **90** 296 (2006)
136. J W Moreau, P K Weber, M C Martin, B Gilbert, I D Hutcheon, J F Banfield *Science* **316** 1600 (2007)
137. D J Burleson, M D Driessen, R L Penn *J. Environ. Sci. Health, Part A* **39** 2707 (2004)
138. B M Simonet, M Valcárcel *Anal. Bioanal. Chem.* **393** 17 (2009)
139. M Valcárcel, B M Simonet, S Cárdenas *Anal. Bioanal. Chem.* **391** 1881 (2008)
140. V N Paunov, O J Cayre, P F Noble, S D Stoyanov, K P Velikov, M Golding *J. Colloid Interface Sci.,***312** 381 (2007)
141. K BéruBé, D Balharry, K Sexton, L Koshy, T Jones *Clin. Exp. Pharmacol. Physiol.,* **34** 1044 (2007)
142. R D Handy, R Owen, E Valsami-Jones *Ecotoxicology* **17** 315 (2008)
143. C Medina, M J Santos-Martinez, A Radomski, O I Corrigan, M W Radomski *Br. J. Pharmacol.* **150** 552 (2007)
144. B Gulson, H Wong *Environ. Health Perspect.* **114** 1486 (2006)
145. *Draft Opinion of the Scientific Committee on the Potential Risks Arising from Nanoscience and Nanotechnologies on Food and Feed Safety* (Parma, Italy: European Food Safety Authority, 2008) p. 35
146. *SCENIHR. Scientific Committee on Emerging and Newly-Identified Health Risks. Opinion on the Appropriateness of the Risk Assessment Methodology in Accordance with the Technical Guidance Documents for New and Existing Substances for Assessing the Risks of Nanomaterials* (Brussels: European Commission Health and Consumer Protection Directorate General, 2008)
147. J T Kwon, S K Hwang, H Jin, D S Kim, A Minai-Tehrani, H J Yoon, M Choi, T J Yoon, D Y Han, Y W Kang, B I Yoon, J K Lee, M H Cho *J. Occup. Health* **50** 1(2008)
148. S T Liu, Y Yan, Z L Chen, Y Z Zhang, X Jin *Nan Fang Yi Ke Da Xue Xue Bao* **26** 331 (2006); http://www.j-smucom/pdf2/200603/200603331.pdf
149. E Chambers, S Mitragotri *Exp. Biol. Med. (Maywood)* **232** 958 (2007)
150. D B Warheit, P J Borm, C Hennes, J Lademann *Inhal. Toxicol.* **19** 631 (2007)
151. G E Onishchenko, M V Erokhina, S S Abramchuk, K V Shaitan, R V Raspopov, V V Smirnova, L S Vasilevskaya, I V Gmoshinski, M P Kirpichnikov, V A Tutel'yan *Byull. Eksperim. Biol. Med.* **154** 231 (2012) [d]
152. T A Platonova, S M Pridvorova, A V Zherdev, L S Vasilevskaya, E A Arianova, I V Gmoshinski, S A Khotimchenko, B B Dzantiev, V O Popov, V A Tutel'yan *Byul. Eksperim. Biol. Med.* **155** 204 (2013) [d]
153. F Moussa, S Roux, M Pressac, E Genin, M Hadchouel, F Trivin, A Rassat, R Céolin, H Szwarc *New J. Chem.* **22** 989 (1998)
154. V I Guma, F M Demidov, V A Ivanov, V V Miller *Neitronno-radiatsionnyi Analiz* (Neutron Radiation Analysis) (Moscow: Energoatomizdat, 1984)
155. K V Kotenko, I K Belyaev, Yu P Buzulukov, A Yu Bushmanov, V F Demin, E S Zhorova, V S Kalistratova, N S Marchenkov, P G Nisimov, R V Raspopov, V Yu Solov'ev *Med. Radiol. Radiats. Bezopasn.* **56** (2) 5 (2011) [e]
156. G Frens *Nat. Phys. Sci.* **241** 20 (1973)
157. G A Shafeev, in *Nanoparticles: New Research* (New York: Nova Science Publ., 2008) p. 1
158. R V Raspopov, V M Vernikov, A A Shumakova, T B Sentsova, E N Trushina, O K Mustafina, L V Kravchenko, I V Aksenov, A A Selifanov, G V Guseva, L I Avren'eva, N V Lashneva, G N Ivanova, I V Gmoshinski, V V Bessonov, S A Khotimchenko, V A Tutel'yan *Vopr. Pitan.* **79** (4) 21 (2010)
159. E Casals, T Pfaller, A Duschl, G J Oostingh, V F Puntes *Small* **7** 3479 (2011)

160. M A Dobrovolskaia, A K Patri, J Zheng, J D Clogston, N Ayub, P Aggarwal, B W Neun, J B Hall, S E McNeil *Mol. Pharm.* **5** 487 (2008)
161. V A Tutel'yan, V A Knyazhev, N A Golubkina, N E Kushlinskii, S A Khotimchenko, Ya A Sokolov *Selen v Organizme Cheloveka: Metabolizm, Antioksidantnye Svoistva, Rol' v Kantserogeneze* (Selenium in Human Organism: Metabolism, Antioxidant Properties, Role in Carcinogenesis (Moscow: Russian Academy of Medical Sciences, 2002)

[a] — *Nanotechnol. Russ. (Engl. Transl.)*
[b] — *Mendeleev Chem. J. (Engl. Transl.)*
[c] — *Biophysics (Engl. Transl.)*
[d] — *Bull. Exp. Biol. Med. (Engl. Transl.)*
[e] — *Med. Radiol. Radiat. Saf. (Engl. Transl.)*